ALL-FIBER VIBRATION SENSORS FOR STEEL INDUSTRY

ALL-FIBER VIBRATION SENSORS FOR STEEL INDUSTRY

By

CAPTAIN ANDREA GREENING

B.Sc., rmc (Royal Military College of Canada) 2000

A Thesis

Submitted to the School of Graduate Studies

in Partial Fulfilment of the Requirements for the Degree

Master's of Applied Science

McMaster University

MASTERS OF APPLIED SCIENCE (2009) **McMASTER UNIVERSITY**
(Department of Engineering Physics) **Hamilton, Ontario**

TITLE: ALL-FIBER VIBRATION SENSORS FOR STEEL INDUSTRY

AUTHOR: Captain Andrea M. Greening, B.Sc., rmc

THESIS SUPERVISOR: Dr. Chang-qing Xu

NUMBER OF PAGES: xii, 85

Abstract

This thesis explores the design, fabrication, and experimental application of a variety of all-fiber vibration sensors, based upon a Michelson interferometer design. These sensors can be used to detect vibration in the low frequency regime. It also provides motivation for its use as an inexpensive yet rugged sensor for use in the harsh environment of a steel hot mill as part of an overall preventative/predictive maintenance program since commercially available piezoelectric sensors currently in use have significant reliability problems.

While this work did result in a device that could withstand the steel hot mill surroundings and detect low frequency vibrations, higher sensitivities are expected from further optimized devices.

Acknowledgements

I would like to thank my supervisor, Dr. Chang-qing Xu for the opportunity to join his research group even though the circumstances were not ideal. I will always appreciate his kind generosity in this regard.

A sincere thank-you to Dr. Jian Yang for the efforts he put into this work before, during, and even after his time at McMaster University. I will never be able to forget the hours we spent winding fiber together.

Various members of Dr. Xu's research group helped me along the way and were very friendly lab companions: Dr. Wangou Liang, Mr. Qianyang Xu, Mr. Yi Gan, Mr. Jian Sun, and Mr. Yao Xiao - best of luck in each of your future endeavours.

Doug Bruce, thank-you for so many things during the Dofasco field-testing, not the least of which was sharing a few laughs with me every time Barry fell asleep. To Kevin Hunt, the man who started it all and who has a passion for all things science and engineering, thank-you for mentoring me and for keeping us safe in the hot mill. Next time I will wear a pink hard hat just for you.

A very special thank-you to Dr. Yong Wang for giving me invaluable direction during the writing of my thesis. It would be an understatement to say that he is a very patient and intelligent man.

I would also like to make special mention of the strong support network of friends that I made during my time at McMaster University: to everyone on the

Diamond Lattice team, Eugene Hsu, Shabnam Homampour, and Chadwick Hall - thanks for making it fun.

Most importantly, Daniel McAllister, I thank you for sacrificing so much to be with me here in Canada and supporting my career in the Canadian Forces. I promise I will never, ever consider doing a PhD - for your sake and for mine.

Contents

List of Figures

List of Tables

CHAPTER 1: INTRODUCTION

1.1 Thesis Motivation for a Fiber Optic Vibration Sensor

While studying single-fiber communication structural designs in the early 1970s, researchers discovered that light guided by an optical fiber had the ability to be modulated by perturbations in the surrounding environment and henceforth used as a fiber optic sensor in a whole host of applications [1]. Since then, laboratories around the world have been investigating the possible roles of these sensing mechanisms. The diversity of these fiber optic sensors is quite remarkable. They can be used to monitor temperature, pressure, acceleration, and so on [2]. This thesis will further examine the role of the fiber optic sensor in measuring vibration.

Mechanical vibration can produce a very undesirable effect in the operation of mechanical systems. It can arise for a multitude of different reasons, i.e. due to imperfections associated with the system, or due to external excitations like unsymmetrical heating or turbulent fluid flow in the area [3,4]. However this unwanted vibration occurs, it is typically associated with stress and fatigue failure of different components. It can do other damage as well by loosing off threaded connections, damaging other delicate components, or affecting the health and safety of the people working with the system. It is therefore important that engineers are able to understand, detect, analyze, and do what is necessary to prevent the negative impacts that can arise from unwanted mechanical vibrations [3].

The motivation for this thesis research arose from a request from an industrial steel manufacturer, ArcelorMittal Dofasco. This company uses many pieces of heavy rotating machinery that are critical to their operation and costly to repair or replace. Failure of certain pieces of equipment could even be catastrophic such that the line production would come to a halt and could also create an extremely dangerous environment for the workers. Therefore, it is essential that this equipment be monitored to ensure its proper functioning so that actions may be taken in advance to minimize the negative consequences. Finding a low cost monitoring system would also surely save on labour costs involved with replacing components that have failed unexpectedly and with replacing components prematurely simply because their replacement date has arrived.

The original vibration sensors utilized in the Hot Mill were mechanically based. [1] Even now, there is one such original sensor in use on the Rougher, which is a 'one of' sensor in that once this sensor breaks there is nothing to replace it, save rooting through some museum archives perhaps. For obvious reasons, this is a significant liability. According to vibration specialists at the Hot

---

[1] I am very fortunate to have had the opportunity to spend countless hours in the Hot Mill under the supervision of Kevin Hunt, a specialist on the Hot Mill Health and Safety Committee at ArcelorMittal Dofasco. The information provided herein specific to the Hot Mill has been explained to me through my most educational and entertaining conversations with Kevin.

Mill, these original sensors used fine wire or thread to suspend a cantilever type of device and were very sensitive to low vibrations. Unfortunately, they were also very susceptible to damage from shock loads and excessive vibration [5].

The second generation vibration sensors used in the Hot Mill are piezo-electric based sensors. They are rugged and have an excellent dynamic range. They are also relatively low cost to manufacture. Regrettably, their performance in the low frequency range is not as good as the preceding sensors. As a result, the Hot Mill managers were forced to implement work around diagnostic methods for predicting maintenance requirements in their rotating equipment [5].[2]

Even though the sensors are low cost to manufacture, locating them in certain areas of the Hot Mill, at the run-out table rolls for example, proved costly (upwards of $2000 at each point). Not only that but the average life span of the sensor and wiring was less than a year. The current design has the sensor mounted in stainless steel waterproof pipe housing and all the wiring is contained in a waterproof flexible conduit. This is an attempt to protect the sensor and wiring from the outside area moisture, heat, corrosion, and X-rays. The piezo-electric sensors do not sustain X-rays very well and steam with high chlorides damages the wiring. There also exists equipment in the mill that operates in such a harsh environment that they remain unmeasured at all. These particular pieces

[2] Canadian Patents Database CA 2434745

of equipment have to be pre-emptively replaced long before they are due to fail as part of an overall predictive/preventative maintenance program [5].

From this came the need for a low frequency sensor which can handle the harsh Hot Mill environment. This is why photonic sensors are so interesting since they use light for signal transmission instead [1]. In addition, the sensor proposed in this thesis is mechanical in nature, so the potential for it to operate better at lower frequencies exists [5].

1.2 Thesis Objective

The goal of this thesis work is to develop a fiber optic vibration sensor that will withstand the harsh environment of a steel Hot Mill, that can detect low frequency vibration and to produce plots of the frequency spectrum produced from applying a Fast Fourier Transform on the acquired data.

In this thesis, a compact sensor that uses a cantilever mounted with optical fibers to determine vibration frequency is presented. Interest arose from the commercial steel industry when their conventional sensors could not stand up to the harsh environment of the Hot Mill and were not reliable at low frequencies as desired [5]. As will be described in more detail in Chapter 2, fiber optic sensors are insensitive to EMI, temperature, water, oil, etc., which is the exact environment where the vibration sensors need to work in the Hot Mill [6].

The general device design requirements were outlined by the vibration experts at ArcelorMittal Dofasco that first approached us with this initiative [7]. The prerequisite conditions were originally based on the idea that the sensor would be used to measure vibration in the area of the table rolls, which include both the motor and roll bearings. These machines rotate under 90 rpm. The roll out tables are used to drive hot strip steel through several mill stands, which are driven individually. As the hot strip steel progresses through the mill rolling process, it is compressed and rolled out until it reaches the desired gauge and length [5].

Table 1.1 summarizes the specifications they gave us to use when designing and fabricating our vibration sensor.

Table 1.1. General device design requirements and specifications for the proposed vibration sensor [7].

Requirements	Vibration (Acceleration)
Measurement Range	0 – 2 g's
Frequency response	0 – 5000 Hz
Accuracy	+/- 5% over full range
Repeatability	+/- 5%
Sample Speed	Continuous
Signal Multiplexing	Ideally Multi-drop
Output FOS Cable length	2 ft – 50 ft, user specified
Environmental Range	-30C – 200C

Typical Operating Range	20C – 80C
Max. g force	20 g's
Exposed to Radiant Heat	YES
Exposed to Radiation (Xray)	YES
Exposed to High EMI	YES
Case	Stainless Steel
Mounting Orientation	Any direction

The acceleration measurement range of 0-2 g's is the typical range experienced by the traditional sensors already in place at the roll out table rolls. The maximum g-force constraint of 20 g's is apparently an industrial standard for this type of working environment. The device might be subjected to an increased g outside its normal operating range if it was dropped down the stairs, for example, or if it was attached to a large process machine like the coiler pinch roll frame and something went wrong (i.e. more mass to create more g) [5].

The frequency response requirement is also based on the typical range experienced by the traditional piezoelectric sensors. That said, the end users were really more interested in us being able to produce a sensor that was capable of identifying vibration at low frequencies since that is where the data is located for large, heavy industrial machines and their traditional sensors are not able to provide reliable feedback in that lower end range [5]. Failures in these very large machines usually take time, sometimes days or even years [8]. Early detection for these failures is in the low frequency range [8] and therefore of most interest to those carrying out conditioning monitoring and preventive maintenance in the Hot Mill [5].

The accuracy and reliability requirements refer to the degree of veracity and the reproducibility of the measurements taken [9]. In other words, the measurements taken are allowed 5% error between the actual value of the measurand and the value of the output as well as 5% deviation between the initial output value and all other subsequent output values measured [7]. The figure below illustrates the definition of both accuracy and reliability.

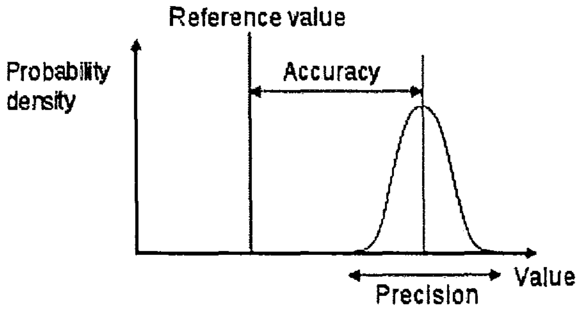

Figure 1.1 The value of accuracy is an indication of the closeness of the measurement to the true value, whereas the value of precision is an indication of the repeatability of the measurement [9]

A continuous reading capability is ideal. However, measurements are typically taken at steady state [5].

The reason behind the requirement to be able to multiplex the sensing system is obvious once one considers that there are 400+ machines to measure, and each machine has four bearings (two per motor and two per roll) [5]. Having individual feeds back to the control room to monitor each of these machines and their individual parts would be cumbersome to say the least and indeed quite unrealistic.

All measurements taken had to occur outside any of the safety barriers surrounding all of the equipment in the mill [10]. As a result, there was a requirement to use extension fibers that were able to reach from the sensing point back past the safety barriers to our setup to allow for measurement during machine operation. This varied from point to point but in practice was generally about 10 to 25 ft.

Since the Hot Mill is a steel building, the operating temperatures inside vary depending on the seasonal temperatures outside. It can be either colder or warmer than outside. This leads to the prediction of the typical operating temperature range. Processing heat takes the operating temperature range up to the high end. However, typical bearings do not go above 120 °C due to grease baking but when a bearing fails it can easily reach temperatures in the 200 °C range. In saying that, if the bearing ever reaches that temperature the survivability of the sensor would be the least of the issues as there would be little to no chance that the bearing would stay inside the machine and imminent structural damage would occur [5].

Radiant heat does come up off the strip of steel as it is processed through the mill. It moves in a straight line and dissipates heat energy upon everything around it. Temperatures are extreme. They vary from 1250 °C at the reheat, 1150 °C at the finisher entrance and are down around < 900 °C in the run out table. Though, these types of temperatures are only ever an issue if the steel product stops moving and saturates the area with heat [5].

The thickness of the steel product is determined with the use of x-rays. Hence, any sensor to be used in this area must be able to withstand x-ray exposure [5].

The majority of motors in the Hot Mill operate DC and therefore produce the associated EMI. In fact, the rougher and the finisher's main drives have so much EMI that no one with a pacemaker is allowed in the vicinity [5].

The Hot Mill environment is basically a 'corrosion bath', hence the necessity to use a stainless steel casing. The chloride in the water there goes over 200 ppm in the spring, and very rarely dips below 100 ppm ever. The water gets drawn into the plant on the east side of the plant, catching the runoff from the neighbouring sewage treatment plant and the salt runoff from the roads also gets into the system and tends to build up as things evaporate. Chlorine is added to the water used in the mill to keep the aerobic and anaerobic bacteria levels down as well [5].

The sensor must also be able to be mounted in such a way that it can monitor acceleration in the X, Y, or Z direction. Ideally, it could measure all three simultaneously [5].

1.3 Thesis Contributions

We had hoped that the main contribution of this thesis work would be in developing a fiber optic vibration sensor that could detect low frequency vibrations and could withstand the harsh environmental requirements detailed in Section 1.2. The analysis of the data acquired from this sensor would be used by engineers to carry out condition monitoring to diagnose machine faults. With this information, they could perform preventative and predictive maintenance that would hopefully minimize downtime of the machine and ultimately lower maintenance costs overall. However, some problems were encountered and that goal proved to be overly ambitious in the time period allotted. We did, however, still make some consequential steps towards that achievement.

Even though the sensor did not produce results that are reliable enough to make the sensor ready for commercial application, it did show potential. Work still needs to be done in certain areas in order to correct the issues that caused difficulties in this round of experiments.

When the sensor was vibrated at a particular frequency and amplitude, in most cases the fundamental frequency was detected. Unfortunately, the harmonic frequencies were detected as well. This is a direct result of using a cantilever that was not optimized for these tests. The cantilever needs to be better characterized so that the appropriate material is selected and employed.

We did produce a sensor that was capable of being field tested at ArcelorMittal Dofasco. The housing and extension fiber was robust and withstood the severe environment with all its dirt, heat, and vibration loads. I learned how to use the sensor and experimental setup for field testing as well.

Additionally, while troubleshooting difficulties with this sensor, other proposals to improve the sensor were developed. Unfortunately, there was not enough time to explore these ideas in great detail as of yet. These include both suggested improvements to the current design as well as a complete change in the sensor design which will be detailed in Chapter 5. This re-design will eliminate the mechanical issue with the cantilever selection and also enable us to very easily multiplex the design allowing us to produce one package that includes three sensors, one for each axis.

1.4 Thesis Overview

The remainder of this thesis is divided into the following chapters:

Chapter 2 presents an overview of fiber optic sensors, how to modulate light in these sensors, different methods used for vibration sensing, and a discussion on why we chose the Michelson interferometer for our sensor.

Chapter 3 describes the vibration sensor device fabrication and experimental application and testing phase details.

Chapter 4 offers up a summary of the thesis work, along with discussion of experimental results.

Chapter 5 will conclude with a discussion of future considerations.

References for Chapter 1

[1]. A. D. Kersey *et al.*, "Application of fiber optic sensors," *IEEE Trans. Comp. Hybrids Manuf. Technol.*, vol. 13, 137 (1990).

[2]. E. Udd., *Fiber Optic Sensors: An Introduction for Engineers and Scientists*, A Wiley-Interscience Publication, 1990

[3]. A.D Dimarogonas *et al.*, *Vibration for Engineers*, Prentice Hall Inc, New Jersey, 1992.

[4] C. Kerr *et al.*, "Optical pyrometry for gas turbine aeroengines," *Sensor Review*, Vol 24, No. 4, 378-286, Emerald Group Publishing Limited (2004)

[5] Private communications and work on-site at ArcelorMittal Dofasco under the supervision of Dofasco Coordinator, Kevin Hunt (2008)

[6] K.T.V. Grattan et al., "Fiber optic sensor technology: an overview," *Sensors and Actuators A: Physical*, vol.82 iss.1-3 (2000)

[7] C.Q. Xu *et al.*, "Progress of FOS for Monitoring of Vibration," submitted for presentation to ArcelorMittal Dofasco (2008)

[8] P.J. Tavner., "Review of condition monitoring of rotating electrical machines," *IET Electric Power Applications*, Durham, UK (2007)

[9] J.R. Taylor, *An Introduction to Error Analysis: The Study of Uncertainties in Physical Measurements*, University Science Books, California, 1982.

[10] Dofasco Safe Work Permit for "Pilot Installation and Testing of Photonics Sensors in Hot Mill," (2008)

CHAPTER 2: INTERFEROMETRY AND SENSING APPLICATIONS IN INDUSTRIAL SYSTEMS

This Chapter serves as an overview of fiber optics in general and of the various classifications of fiber optic sensors. In addition, it will highlight different modulation and de-modulation techniques available for fiber optic sensing systems. The goal of this Chapter is to highlight the thought process behind selecting an appropriate method when setting out to design a fiber optic sensing system. Following that a few examples of industrial fiber optic sensors in use today will be showcased.

2.1 Classification of Fiber Optics

Over the past three decades, fiber optic technology has been an ever-growing field of study. Initially, the rapid growth was due to interest in optoelectronics and fiber-optic communications. Fiber optic sensor technology began in parallel as both industries revolutionized, which ultimately resulted in a higher volume output of their products [1]. Exploration into new techniques like microbending allowed the advance of more efficient optical systems as well [2]. The motivation to replace conventional sensors is obvious when one considers just a few of the fiber optic sensor advantages. Some of their many advantages are that they:

- are unaffected by electromagnetic interference;
- have high sensitivity;
- have a sensing point that requires no electrical power;
- are small;
- are lightweight;
- are able to be multiplexed; and
- are cost-effective to produce in the majority of cases [1,3].

These sensing mechanisms have enormous diversity to be exploited in fields ranging from temperature, pressure, and vibration measurement to liquid levels and chemical detection. Figure 2.1 illustrates some of these primary areas of interest for this technology.

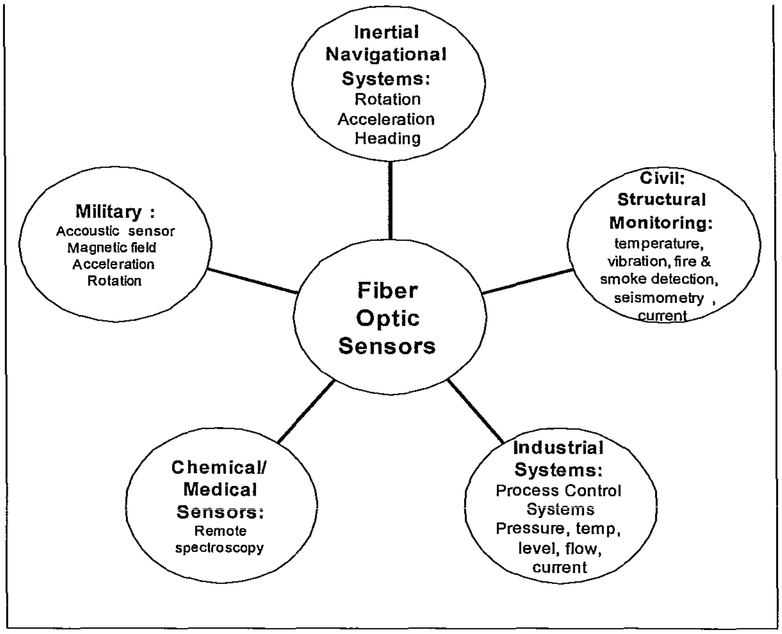

Figure 2.1. Fiber optic sensor areas of application [4].

In general, the fiber optic sensing market is separated into two types, as either intrinsic or extrinsic (see Figure 2.2). According to market research reports in 2008, intrinsic fiber optic sensors hold the largest share of the US market, generating $170.0 million in 2007 and an estimated $238.0 million in 2008. At that time, the intrinsic fiber market was expected to generate $306.0 million in 2009 and $1.4 billion in 2014. Alternatively, the extrinsic fiber optic sensor division was worth $65.0 million in 2007 and an estimated $92.0 million in 2008. The forecast in 2008 was that it would increase to $124.0 million in 2009 and $219.0 million in 2014, which is still a hefty annual growth rate even though it is much smaller than that of its intrinsic counterpart [5].

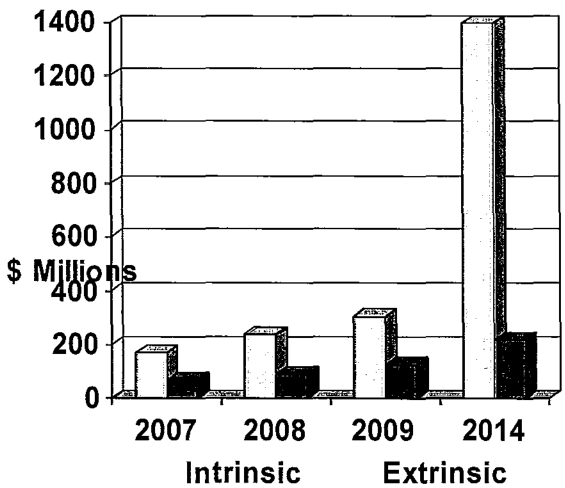

Figure 2.2. US Market for fiber optic sensors, by type, 2007-2014 ($ Millions) [5]

2.1.1 Intrinsic fiber optic sensors

An intrinsic fiber optic sensor, by definition, is one where all the sensing of the environmental effect takes place within the fiber. It is also commonly referred to as an "all-fiber" sensor.

In 2008, Ref [6] gave an account of characteristic phase changes that can be detected using intrinsic fiber optic sensors. They reported that phase changes of about 100 radians per meter per °C temperature change, 10 microradians per meter per $\mu\varepsilon$ of longitudinal strain and 10 microradians per meter per bar of pressure change could be detected, although exact numbers will vary somewhat with fiber type and wavelength of operation [6].

One remarkable example is the fiber optic gyroscope (see Figure 2.3), which was first proposed in 1975 and is enabled through the Sagnac effect (see section 2.2.2). Advancements in this domain led to usage in many areas including fly-by-light military and commercial aircraft applications starting around 1999 and in some land based vehicle models beginning about 1993. Other areas of interest for the fiber optic gyroscope are missile defence and commercial ships' navigation [7].

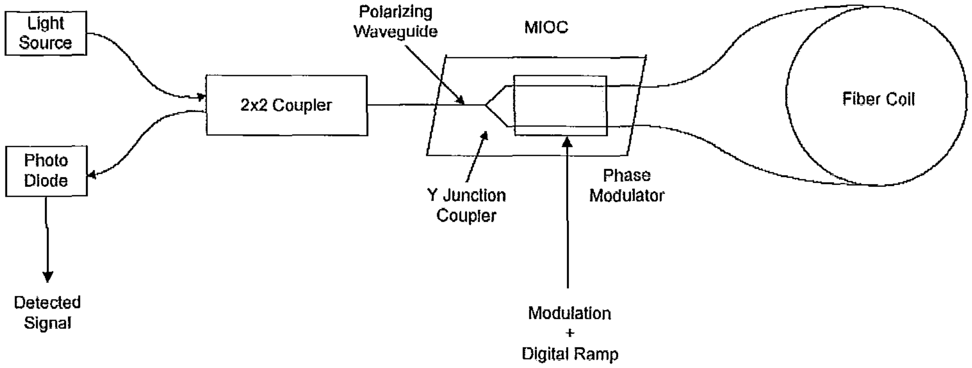

Figure 2.3. Optical Schematic of a Typical Fiber Optic Gyroscope [7]

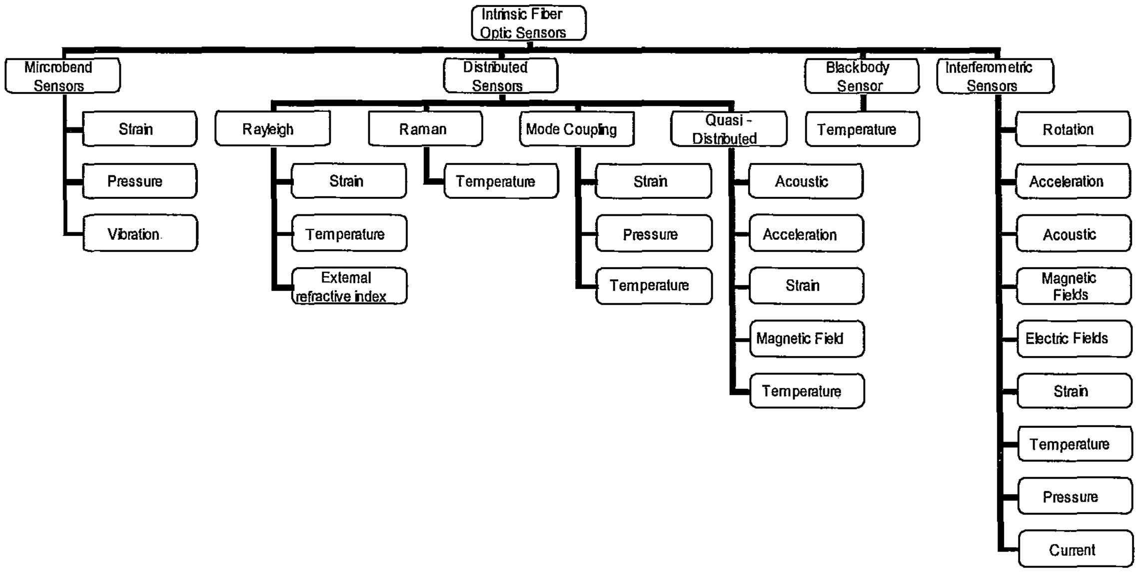

Figure 2.4. Intrinsic fiber optic sensors [2].

Figure 2.4 illustrates many of the intrinsic fiber optic sensors and their field applications. The interferometer systems to be described in part 2.2.2 of this Chapter are a significant subclass of intrinsic fiber optic sensors. The list of examples in this category is extensive.

2.1.2 Extrinsic fiber optic sensors

Extrinsic fiber optic sensors differ from their intrinsic counterparts because extrinsic, or hybrid fiber optic sensors incorporate a sensing region outside of the fiber. The fiber is used to deliver the light to and from the sensing area. An example would be when the light beam traversing the fiber is used to power an electric sensor and subsequently used to return the data via a fiber optic data link, hence the term "hybrid" sensor. Figure 2.5 shows a diagram illustrating many of the extrinsic or hybrid fiber optic sensors and their applications.

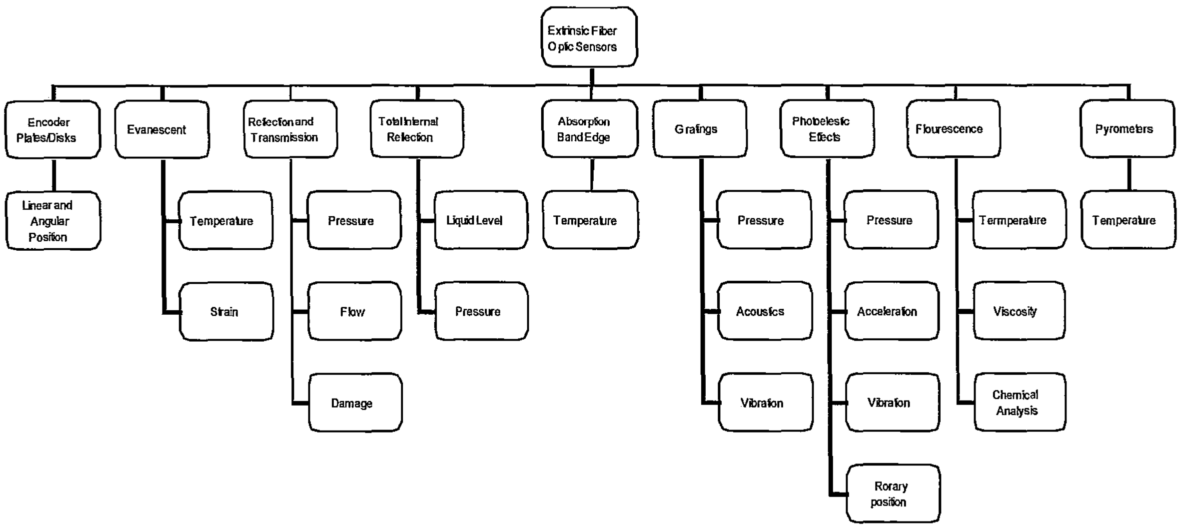

Figure 2.5. Extrinsic Fiber Optic Sensors [2]

An interesting example of an extrinsic fiber optic sensor is the one used to measure temperature inside jet engines. These sensors use fiber to transmit radiation into a radiation pyrometer located outside the engine whose output is used to determine the temperature inside the engine. This device is commonly referred to as the optical pyrometer for gas turbine engines (see Figure 2.6). It is a critical component since turbine engines work best when they are operated at the highest turbine entry temperature. However, temperature must be monitored in order to increase the turbine blades' lifetime since it is their metallurgic specifics that limit the highest turbine temperature possible [8]. As fuel prices continue to rise, no doubt so does the interest in improving the fuel efficiency of the turbine engine.

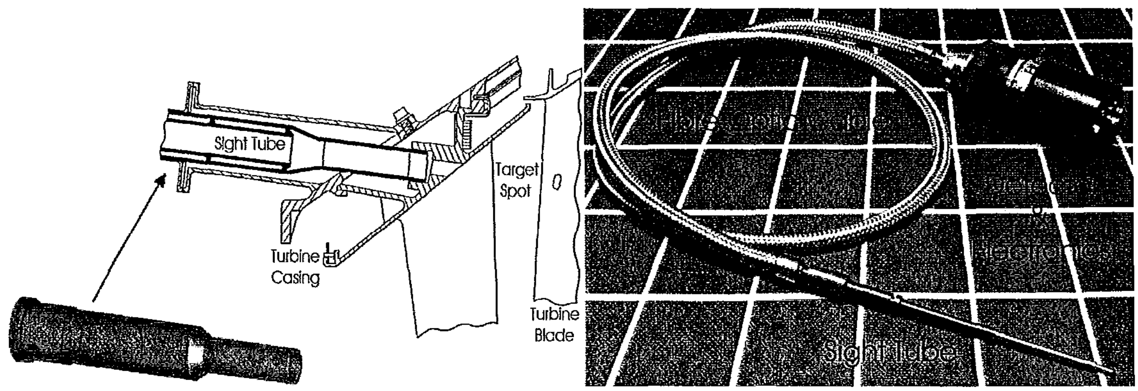

Figure 2.6. The image on the left illustrates the direct viewing of an installed optical pyrometer. The image on the right shows the optical pyrometer components [8].

2.2 Modulation

Modulating a light source is a process by which information is impressed onto the light source, called the carrier for efficient transmission [9]. Virtually any environmental effect, such as temperature, pressure, or strain, etc., can be converted to an optical signal, modulated, and then interpreted. It is also possible that there are many sensor types that could measure the same environmental effect. The crucial step is often in choosing the appropriate method and designing a suitable sensor so that only the desired environmental effect is detected and measured [2].

If the carrier has a voltage wave:

$$e(t) = A_c \sin(\omega_c t + \phi_c) \qquad \text{(Equation 2.1)}$$

where A_c is the amplitude, ω_c is the angular frequency, and ϕ_c is the phase angle of the light source, then any change of any of those parameters would represent a modulation process [9].

In other words, there are four ways to perform modulation:

2.2.1 Amplitude (intensity);

2.2.2 Frequency;

2.2.3 Polarization; and

2.2.4 Phase (also labelled 'interferometric').

2.2.1 Amplitude or Intensity-based fiber optic sensors

If the amplitude, A_c, is varied in relation to ω_m, or the modulation frequency, while keeping the other parameters constant at the same time, Equation 2.1 becomes:

$$e(t) = A_c(1 + m_a \cos \omega_m t) \sin(\omega_c t + \phi_c)\ ) \qquad \text{(Equation 2.2)}$$

From here the amplitude modulation process can be recognized from the following equation:

$$e(t) = A_c \sin \omega_c t + \frac{m_a A_c}{2} \cos(\omega_c - \omega_m)t - \frac{m_a A_c}{2} \cos(\omega_c + \omega_m)t \qquad \text{(Equation 2.3)}$$[3]

where the modulation index, m_a, is defined as the amplitude ratio of the modulation signal to the carrier amplitudes (A_m/A_c). The resulting equation consists of the original carrier plus upper and lower side bands [9].

Common concepts involved with intensity based sensors and intensity modulation are microbending, transmission, and reflection [10]. Intensity based sensors are simple in that they do not require much in the way of interface electronics.

[3] ϕ_c has been omitted for the sake of simplicity.

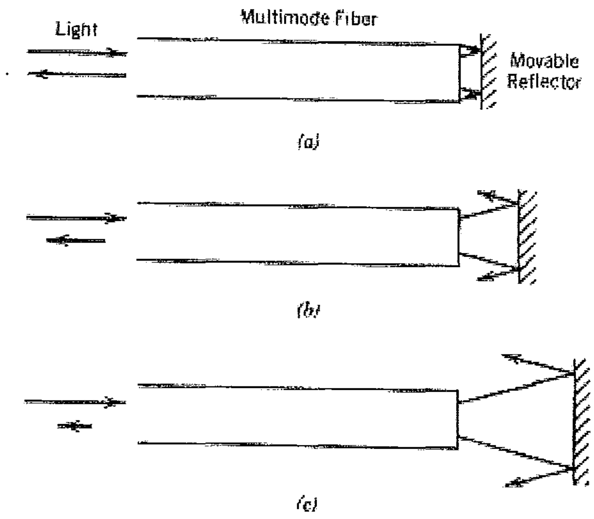

Figure 2.7. Single fiber optic sensor with a moveable mirror. The intensity varies with light loss [2].

In a basic intensity sensor set-up, like the one illustrated in Figure 2.7, light travels through the fiber until it leaves through the end of the fiber in a cone pattern and hits a mirror. If the mirror is close to the end of the fiber, most of the light will be coupled back into the fiber (a). If the mirror is far from the end of the fiber, less light will be reflected back, (b) and (c). The relationship between the fiber and mirror distance and the amount of light reflected back may be used to measure distance.

However, as with most intensity sensors, the lack of a reference signal limits the system. For example, a change in light source intensity during the scan could cause an incorrect distance measurement [2]. Microbending in the leads to and from the sensing region can also be a source of error in the system if the leads move while the sensor is in operation [10].

Figure 2.8 illustrates typical optical fibers and their effect from bending. It is evident from this plot that the large-core plastic-clad silica (PCS) fibers and hard polymeric-clad silica fibers are the least sensitive to bending loss and therefore best suited to be used as sensor leads when microbending needs to be taken into account [10].

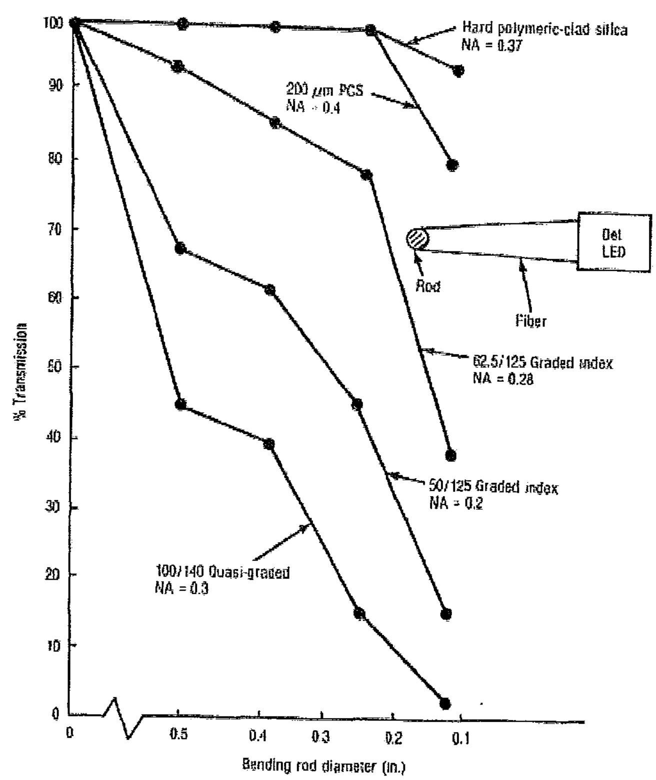

Figure 2.8. Percent transmission vs. bending for different optical fibers [10]

Even though intensity modulated based sensors have some limitations, they do have significant usage in digital applications when used as switches and counters [10]. They have also been used extensively in displacement, temperature, and pressure sensing applications in both military and industrial environments once compensated detection systems for variations in light-source intensity and microbending were incorporated [10]. Figure 2.9 illustrates other sensing mechanisms under the umbrella of intensity-based sensing techniques.

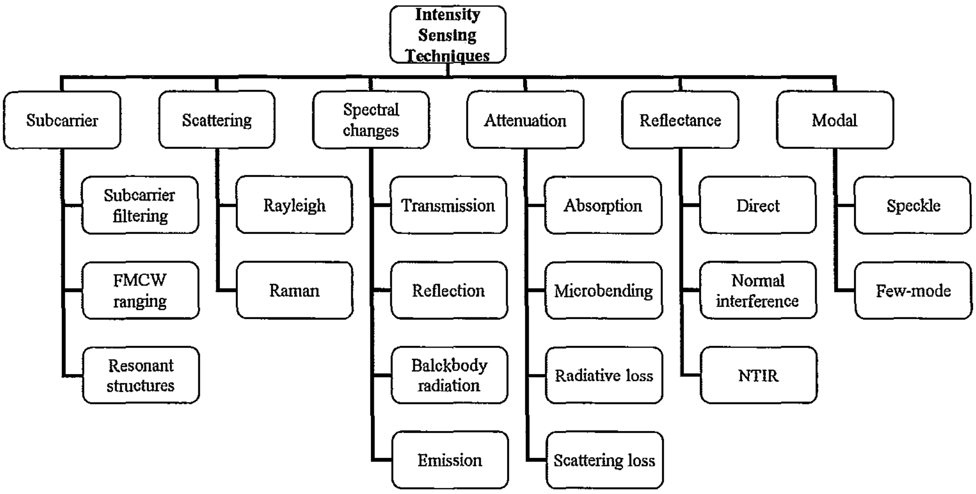

Figure 2.9. Intensity-based sensing techniques [4]

One example similar to the concept illustrated in Figure 2.7 is the amplitude-modulated optical fiber displacement sensor, whose sensor head is shown in Figure 2.10. This sensor is designed to measure vibration. This sensor operates oppositely from the one illustrated in Figure 2.7 but is still an intensity-based sensor. This sensor uses an emitting fiber and receiving fibers so that when the distance to target, z, is zero no light gets coupled into the receiving fibers since all the light is coupled back into the emitting fiber. As z increases, a rising amount of the light gets coupled into the receiving fiber up until the point where the peak intensity is reached [11].

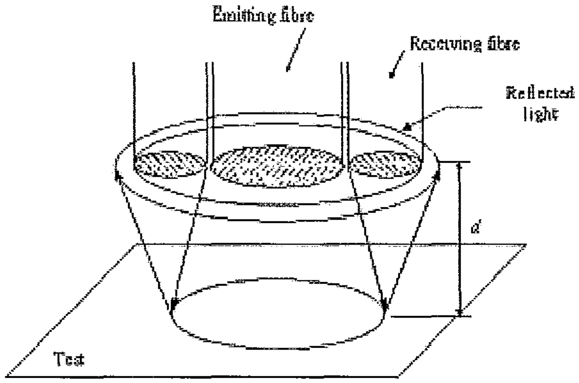

Figure 2.10. An amplitude-modulated fiber optic displacement sensor head [11].

Further to that, a portion of the experimental setup of the amplitude-modulated fiber optic displacement sensor being used as a vibrometer is illustrated in Figure 2.11.

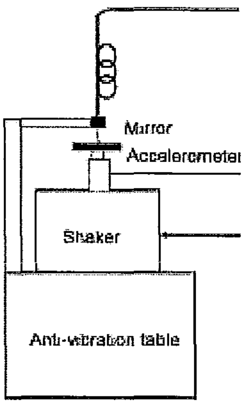

Figure 2.11. Experimental setup of the amplitude-modulated fiber optic displacement sensor used as an optical vibrometer (showing only the sensor end of the set-up) [11].

The mirror is mounted on an accelerometer, which is in turn mounted on the shaker table. The sensor will be used to sense displacement changes in the mirror positioning and then analysed to produce the vibration spectrum [11].

2.2.2 Frequency Modulation

If the frequency is varied while keeping the other parameters constant at the same time, Equation 2.1 becomes:

$$e(t) = A_c(1 + \sin(\omega_c + m_f \sin \omega_m t)) \qquad \text{(Equation 2.4)}$$

where m_f is the modulation index $\left(\frac{\Delta w}{w_m}\right)$, [9].

Frequency modulated sensors may utilize the Doppler Effect to perform very sensitive detection of moving objects and are used today as both electrical and acoustical radars. They can also be used to measure free vibration as seen with the fiber optic laser-Doppler vibrometer, for example, which can be used in the prevention of serious damage to the hull, keel, deck, and/or bow of marine structures. In this case, the advantages are that the laser-Doppler vibrometer has a simple structure and also that there is theoretically no limit on the gauge length, which is important when applied to marine structures where overall length sometimes exceeds 200 m [12].

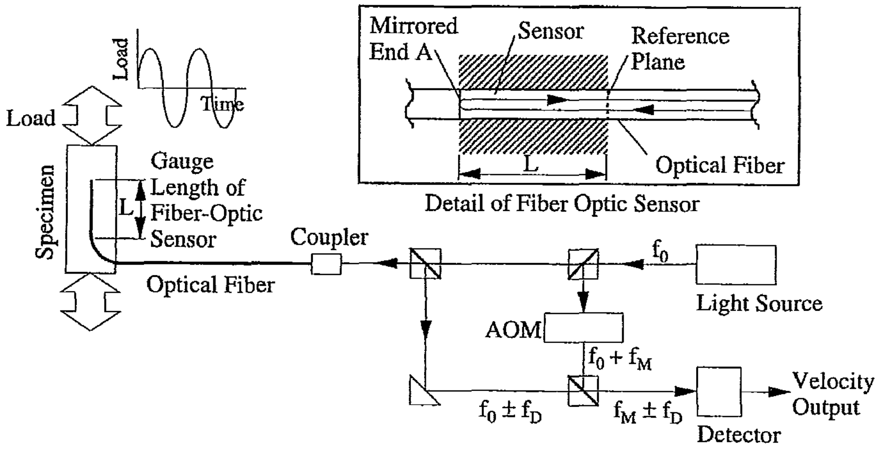

Figure 2.12. Set-up of a laser-Dopper vibrometer [12].

With a laser-Doppler vibrometer set-up (Figure 2.12), the extension and compression of the fiber is measured. The frequency shift, f_D, between the reference plane and the reflected light from the fiber end, relates to the relative displacement rate along the gauge length, L, of the fiber, $\upsilon = dL/dt$. The frequency shift is given by:

$$f_D = -2\upsilon/\lambda \qquad \text{(Equation 2.5)}$$

The reflected laser beam has a frequency change from f_0 to ($f_0 \pm f_D$) whereas the reference beam has a modulated frequency of ($f_0 + f_M$). The reflected beam interferes with the reference beam and this interference signal is then detected with the detector and has a frequency of ($f_M \pm f_D$). Following that the Doppler shift of f_D is able to be measured [12].

2.2.3 Polarization Modulation

The birefringence properties of optical fiber can be influenced by electrical, magnetic, and mechanical means. In other words, the state of polarization of the light within the fiber can be influenced by these physical phenomena. The advantage of using a polarization modulated sensor is primarily that the light is confined within a single fiber rather than requiring a reference arm. Therefore, the polarization components are simpler to analyze when compared to interferometric devices. On the other hand, the system is further complicated by the requirement to have one polarizer at the input end of the fiber to bring in light of one polarization and one at the output end to separate the polarization components for delivery to the detectors [9].

Figure 2.13 is an example of a polarization modulated sensor. A laser sends light through a polarizer and into a fiber that is coiled around a small cylinder that expands and contracts as a reaction to acoustical pressure waves. As the cylinder reacts to the environmental changes, the fiber will sense a strain from the change in the pressure on it. Birefringence is induced by strain on the fiber, which in turn changes the index of refraction of the fiber. This birefringence results in independent propagation of two linearly polarized eigenmodes. The result is detected as a change in intensity from the polarization rotation of the light propagating in the fiber [9].

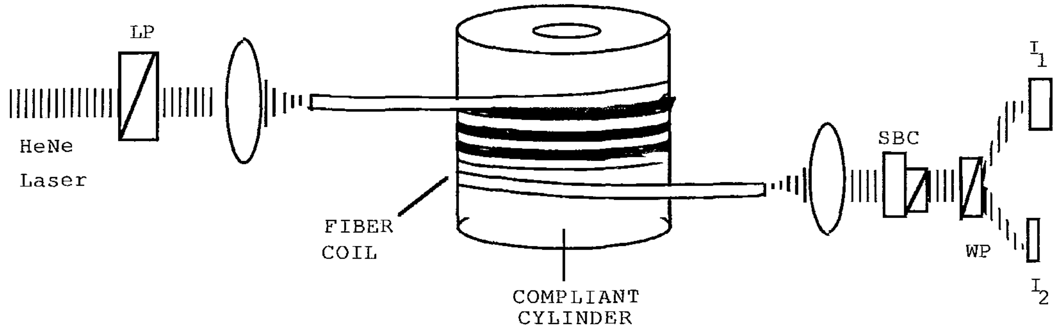

Figure 11.6 An induced birefringence pressure sensor. After S. C. Rashleigh [10].

Figure 2.13. An induced birefringence pressure sensor [9]

In the same manner as described above, other environmental changes can be sensed by simply changing the cylinder. For example, if the cylinder were made from a magnetostrictive material, then it would sense changes to the magnetic field or current or if the cylinder changed size in response to temperature variations for instance [9].

2.2.4 Phase-modulated based fiber optic sensors

As will be outlined in Table 1 further along in this Chapter, phase-modulated sensors provide high sensitivity to a varying number of environmental changes, including strain, electric and magnetic fields, and rotation to name only a few [4,9]. As a result of their high sensitivity, very high resolution measurements are therefore possible. Phase-modulation involves the measurement of the light path of the fiber in terms of the phase angle [9].

The frequency spectrum of a phase-modulated system is that from frequency modulation. An expression for a phase-modulated system can be presented as:

$$e(t) = A_c(1 + \sin(\omega_c + m_p \sin \omega_m t)\,) \qquad \text{(Equation 2.6)}$$

where m_p is the modulation index $\left(\frac{\Delta q}{q_m}\right)$, [9].

Characteristically, phase-modulated sensors will employ a coherent laser light source, typically a diode laser, which is coupled into a single mode fiber and then split between two fiber arms using a fiber coupler. If the environment perturbs the fibers in reference to one another a phase shift can be detected with great accuracy. This type of device is known as an interferometer [4,10]. Phase-modulated sensors can be extremely precise, more so than intensity-based fiber optic sensors. However, their increased sensitivity often comes at a higher price financially [10].

There are four commonly utilized configurations of interferometers:

i. Mach-Zehnder;

ii. Michelson;

iii. Fabry-Perot; and

iv. Sagnac. [10]

In a Mach-Zehnder interferometer (see Figure 2.14), the coupled light is split equally between a signal or sensing arm and a reference arm, which does not come in contact with the measurand.

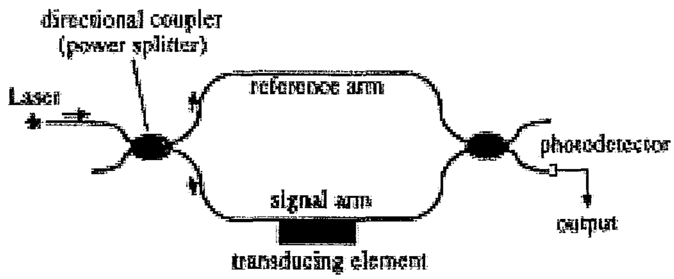

Figure 2.14. Make-up of a phase-modulated sensor using fiber optic Mach-Zehnder interferometer [4]

The signal arm is usually bonded to or coated by a measurand responsive material such that the fiber is strained when the material responds to the measurand. A second fiber coupler is used to recombine the light from the two arms and this signal is sent to a photodetector. The phase of the light in a sensing fiber arm is then compared to the phase of light in a reference fiber arm. Any change in length (or index of refraction) of the sensing arm in turn changes the optical phase of the light. The relationship between the optical phase shift and change in length of the sensing arm is:

$$\Delta\phi = \beta\Delta L + L\Delta\beta \qquad \text{(Equation 2.7)}$$

where L is the length of the fiber, $\beta=2\pi n/\lambda$ is the propagation constant, and n is the index of refraction of the fiber core [4].

The Michelson interferometer shown in Figure 2.15 is similar to the Mach-Zehnder interferometer but is made less complex by taking away the requirement for a second fiber coupler. Instead, the ends of the signal and reference arms are mirrored at their ends. The light is reflected back through the two arms, through the initial beamsplitter where it is recombined and sent to a photodetector. Since the optical beam travels through the fibers twice, the optical phase shift per unit length is doubled. Although the Michelson interferometer is a simpler version of the Mach-Zehnder interferometer, it is more vulnerable to reflection induced instabilities in the source because it is operated in a reflective mode. However, this problem can be essentially overridden by using an incoherent source [6].

The optical intensity out of the sensor is a function of the relative phase shift as can be seen in Figure 2.16. When the phase shifts are an integral number of half wavelengths (phase shift = π, 3π, ...), the light from the two interferometer arms interfere destructively and have minimum intensity. Oppositely, at integral numbers of wavelength (phase shift = 0, 2π, 4π, ...), the light constructively interferes providing maximum interference. However, the region of most interest is at the ¼ wavelength shift ($\pi/2$, $3\pi/2$) where the rate of change of intensity with phase shift is the largest and therefore, the most sensitive [10]. In other words, referring once again to Figure 2.16, if the phase is varied and we are operating in the area of a peak or trough, the output intensity is small. On the other hand, if the phase is varied by the same amount at the linear part of the curve then the variation in the output intensity is much higher. Hence, the sensitivity of the interferometer is highest at this linear part of the curve.

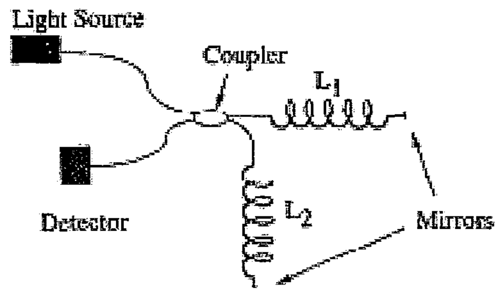

Figure 2.15. The fiber-optic Michelson interferometer configuration [1]

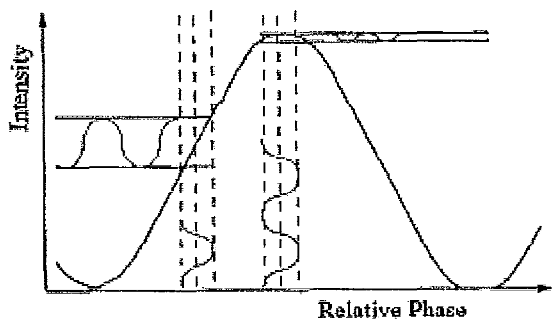

Figure 2.16. The sensitivity of the Mach-Zendner and Michelson interferometers varies with the relative phase between the two light beams, or arms [1].

Unlike the Mach-Zehnder and Michelson setups, the Fabry-Perot interferometer does not have a reference arm (see Figure 2.17). Instead has two parallel mirrors separated by an air cavity, which can be several millimetres to several centimetres in width. Since the light reflects back and forth between the two highly reflective mirrors it experiences phase delay in the cavity many times. For a particular θ, when one mirror is moved, the wavelength of light that produces constructive interference changes and the system acts as an interferometer. Also, since there is a relationship between the angle of refraction and the index of refraction, it is also possible to create a Fabry-Perot interferometer with a constant d by varying the pressure of the gas inside the cavity between the two mirrors [2,13].

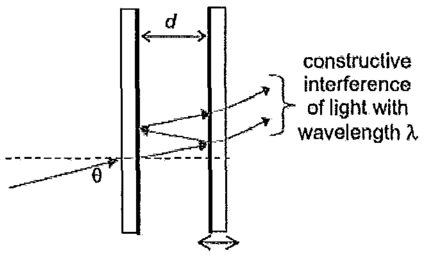

Figure 2.17. The Fabry-Perot interferometer configuration [13]

In the case of a fiber optic Fabry-Perot fiber interferometer (Figure 2.18), the phase delay is introduced from the interference between the optical beam that is reflected (about 95% reflected, 5% transmitted) from the end face of the fiber and the reflected beam from the mirror [10,13]. Generally, Fabry-Perot sensors are twice as sensitive as Mach-Zehnder and Michelson sensors [10].

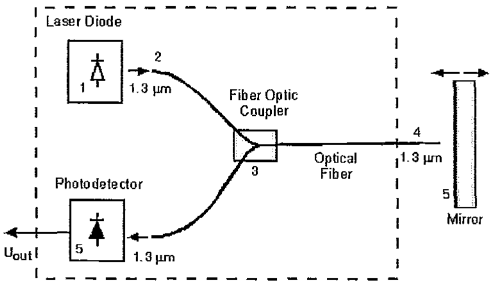

Figure 2.18. The fiber optic Fabry-Perot interferometer configuration [14]

The Sagnac interferometer takes into account a phenomenon known as the Sagnac effect. In this case, the interferometry is brought about through rotation. The incoming light is split between too arms and is made to travel in opposite directions around a ring (see Figure 2.19). The ring is constructed in such a way that it is able to rotate. If the ring of radius R is rotating in a clockwise direction at rate Ω, the clockwise beam travels a length equal to $2\pi R + \Omega R\Delta t$ and the counter clockwise beam traverses a path of length $2\pi R - \Omega R\Delta t$. In other words, one of the beams covers more distance than the other and therefore takes longer to return to the entry point. The two counter propagating beams of light create an interference fringe pattern when they meet up on return to the entry point. The fringe pattern position is a function of the angular velocity of the ring [2].

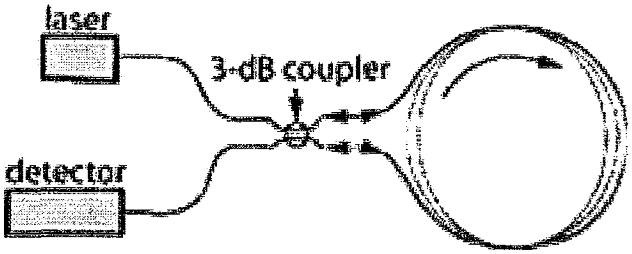

Figure 2.19. A fiber optic Sagnac interferometer configuration. Rotation of the fiber coils causes a phase shift in the combined output at the detector [15].

It is very difficult to use the Sagnac interferometer for vibration measurements so its potential in this regard will not be debated or examined further than the previous general description.

2.2.5 Choosing the appropriate method

Fiber optic sensors really start to look their best when they have specialized applications [3]. As was previously described in Chapter 1 of this thesis, although there are advantages to using piezo-electric sensors for vibration sensing in the hot mill, there are also many disadvantages. For this reason, an extrinsic fiber optic sensor which uses fiber to deliver the light to and from the traditional sensor head would not provide the additional robustness required to withstand the harsh environment within the hot mill. It also does not resolve the difficulties of diagnosing vibration problems in the low frequency range. Consequently, finding a solution using intrinsic fiber optic technology was chosen as the method of choice for this particular vibration sensor.

Table 2.1 lists the main areas for fiber optic sensor application. It can be inferred from Table 2.1 that development in the area of intensity-based fiber optic sensors has been directed more toward lower cost process-control type applications. On the other hand, phase modulated sensor development has been more for high performance or high sensitivity sensors like those used in inertial navigational units and geophysical applications for example [4].

Table 2.1: Principle Application Areas for Fiber Optic Sensors [4]

Intensity-Based Sensors	**Phase-Modulated Sensors**
Temperature	Strain
Pressure	Pressure
Force	Acoustic fields
Flow	Magnetic fields
Liquid level	Electric fields
Position (displacement)	Rotation (gyroscope)
Vibration	Acceleration
Turbidity (oil pollution)	Vibration
Chemical	Velocity
Radiation	Temperature
Humidity	Flow
	Current

Since high sensitivity and resolution can be found using a relatively simple set-up, phase-modulation was the technique chosen for the low frequency vibration detection scheme employed in this thesis. Overall, the Michelson approach provides a straightforward design that can be fairly easily packaged for our experiments. In addition, the Michelson interferometer allows for uncomplicated multiplexing possibilities which will be useful for further development of a distributed system in the future.

2.3 Interferometric sensing – Demodulation

To achieve extrinsic phase modulation in all-fiber devices the fiber must be either stretched or squeezed by some external means. When considering two-beam interferometry, very small differential phase shifts can be detected and measured. Even though this type of sensor is very sensitive, there are disadvantages to using this type as well including the presence of pressure fluctuations and low frequency random temperature fluctuations experienced by the interferometer arms. Unfortunately, these experiences are sometimes nontrivial and can cause signal fading or signal distortion, also known as frequency up-conversion. Several detection schemes do exist to help combat these issues [16]. In the case of this thesis, no such demodulation scheme was employed. For future reference it is worthwhile to briefly mention them here.

The earliest example of interferometric demodulation applied to the tracking of phase changes is the active homodyne tracking. It would not be practical to base our sensor system on this principle since active homodyne tracking requires an electronically driven element in the sensor system to change the interferometer conditions [17]. This is impractical for our application at the Hot Mill because of the environment. It would be counter-productive to build an all-optical device and then include electronics back into the system.

Another approach is a laser frequency modulation technique, which includes the phase-generated carrier approach. This method improves detection accuracy and simplifies the required electronics [16].

The variation of the light intensity at the output from the sensor will be:

$$I(t) = A + B\cos\phi(t) \qquad \text{(Equation 2.10)}$$

where $\phi(t)$ is the optical phase difference between the optical paths of the two sensing arms. A and B are constants that are proportional to the input power [17]. In this technique, initially a high-frequency carrier phase signal with fixed amplitude is generated by applying a current modulation carrier signal, $\Delta i \sin(\omega_c t)$, to the laser source of the sensor [16]. This action generates a carrier phase signal of $\Delta\phi(t)$, which can be expressed as:

$$\Delta\phi(t) = \Delta\phi_o t \qquad \text{(Equation 2.11)}$$

where $\Delta\phi_o = [\frac{2\pi\Delta Ln}{c}] \times \Delta i \times (\frac{\delta v}{\delta i})$. Therefore, once the carrier phase signal is added, Equation 2.10 becomes:

$$I(t) = A + B\cos[\phi(t) + \Delta\phi_o \sin\omega_c t] \qquad \text{(Equation 2.12)}$$

such that Equation 2.12 includes the influence from the carrier phase signal and the environmental effects as well [16].

Using Bessel functions, Equation 2.12 may be expanded to reveal that:

$$I(t) = A + B\{[J_o(\Delta\phi_o) + 2\sum_{n=1}^{\infty} J_{2n}(\Delta\phi_o)\cos 2(n\omega_c t)] \times \cos\phi(t) - [2\sum_{n=0}^{\infty} J_{2n+1}(\Delta\phi_o)\sin((2n+1)\omega_c t)] \times \sin\phi(t) \qquad \text{(Equation 2.13)}$$

From Equation 2.13 comes the amplitude $S_1(t)$ in I(t) at the fundamental carrier and $S_2(t)$ in I(t) at the second-harmonic carrier, which are given by Equations 2.14 and 2.15 respectively [16].

$$S_1(t) = -BJ_1(\Delta\phi_o)\sin\phi(t) \qquad \text{(Equation 2.14)}$$

$$S_2(t) = -BJ_2(\Delta\phi_o)\cos\phi(t) \qquad \text{(Equation 2.15)}$$

Figure 2.20 illustrates the 'differentiate and cross-multiply demodulator', which gives the optical phase difference when demodulated from Equations 2.14 and 2.15.

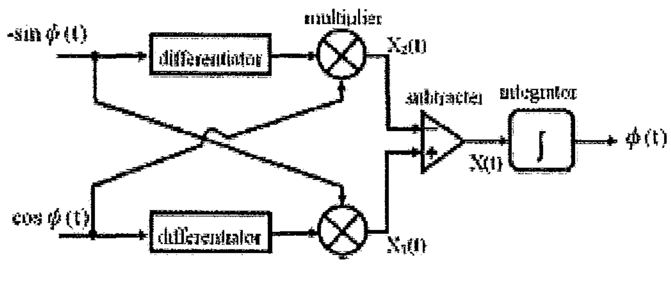

Figure 2.20. Schematic of the interferometric phase-shift demodulator [16]

2.4 Recent Examples of Fiber Optic Sensors utilized in Industrial Domains

There is a nearly infinitesimal range of possibilities for fiber optic sensor exploitation. There exist hundreds of small market sectors each with their own unique measuring requirements that could adopt new fiber optic sensing techniques [6]. In view of the fact that the scope of this thesis originated from a request from the local steel industry in Hamilton, Ontario, this discussion of recent advancements in fiber optic sensor technology will be limited to a few found in other industrial domains, namely intrinsic sensors focused predominantly on physical measurands that have already seen considerable market penetration. As seen in Figure 2.1, fiber optic sensors employed in the industrial arena include but are not limited to pressure, temperature, level, flow, and other process control sensors [4].

As described in section 2.1, fiber optic sensors are a desirable technology to many industries because of their robust nature in many diverse and harsh environments. Particularly, they are immune to electromagnetic interference, are lightweight, sensitive, and are reasonably inexpensive to manufacture and maintain.

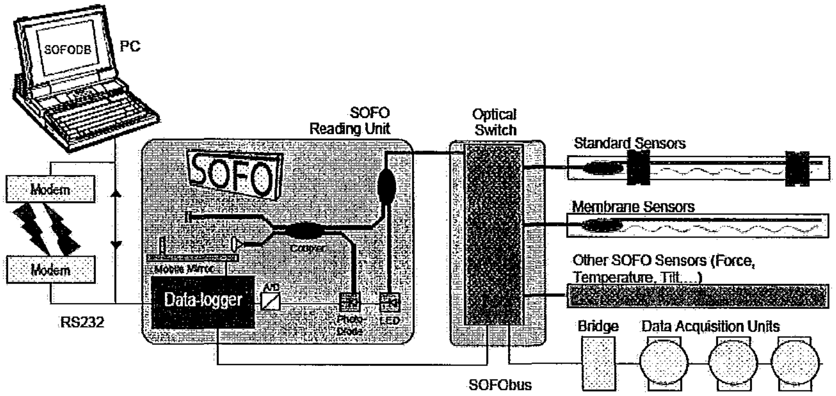

Figure 2.21. SOFO measurement technique using low-coherence interferometry [18]

One such fiber sensor that has been in use for over a decade is the Michelson interferometric extensometer used to monitor relative movements between two points in a structure. Figure 2.21 illustrates one such measuring system.

The LED emission is launched into the fiber and directed, through a coupler, and into the two fibers which are mounted on or embedded in the structure to be monitored. One of the fibers remains in mechanical contact with the structure so that it experiences the same deformation as the structure itself. The other is the reference fiber, which remains free from contact with the surface. The light is reflected back from mirrors at the end of the fibers, is recombined at the coupler, and subsequently processed to determine the path difference. Each measurement reveals data pertaining to the deformation of the structure [18].

Optical fiber vibrometers have many different uses as well, one of which was briefly described in Section 2.2.2 of this Chapter – the laser-Doppler vibrometer. To name only a few, there exist scanning, high speed, in plane, and rotational vibrometers in use in all kinds of commercial applications like the automotive and aerospace industries [19].

Scanning vibrometers can be set up to scan entire surfaces to help resolve noise and vibration issues. Figure 2.22 illustrates one such scan of engine components on a vehicle. In this case, the scanning vibrometer is also a high-speed vibrometer that allows vibration measurements up to 20 m/s. Although, there do exist other vibrometers that can measure vibrations at speeds even higher than that [19].

Figure 2.22. Scanning vibrometer in operation [19]

The difference between in-plane and rotational vibrometers is obvious in the name. In-plane vibrometers measure continuous velocity and variable components that are perpendicular to the central axis of the two converging light beams (like the laser-Doppler vibrometer) and is not only used in measuring free vibration on marine structures but can also be used to study devices like belt drives, ultrasonic knives and scalpels, where slippage and vibration are problematic [19].

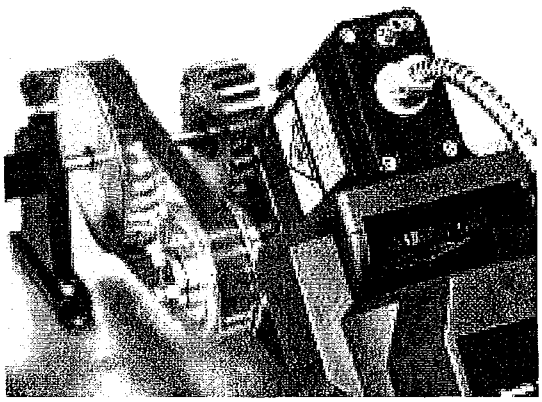

Figure 2.23. Rotational vibrometer on a belt drive [19]

On the other hand, rotational vibrometers are important when measuring rotating structures like crankshafts, axles and pulleys. Figure 2.23 shows a rotational vibrometer being used to measure rpm, angular velocity and angular displacement on a belt drive. It serves to help designers reduce noise and vibration and reduce rotational fatigue of the components. Both in-plane and rotational vibrometers are incredibly important for developing more reliable vehicles and aircraft systems [19].

References for Chapter 2

[1]. E. Udd., "An overview of fiber-optic sensors," *Rev. Sci. Instrum.* 66 (8), (1995)

[2]. E. Udd., *Fiber Optic Sensors: An Introduction for Engineers and Scientists*, A Wiley-Interscience Publication, 1990

[3] A.D. Kersey., "A Review of Recent Developments in Fiber Optic Sensor Technology," *Optical Fiber Technology* 2, 291-317 (1996)

[4] A. D. Kersey *et al.*, "Application of fiber optic sensors," *IEEE Trans. Comp. Hybrids Manuf. Technol.*, vol. 13, 137 (1990).

[5] http://www.bccresearch.com/pressroom/IAS002D.html

[6] B. Culshaw., "Fiber-Optic Sensing: A Historical Perspective," *Journal of Lightwave Technology*, Vol 26, No. 9, (2008)

[7] G.A. Pavloth., "Fiber-Optic Gyros: The Vision Realized," Northrop Grumman

[8] C. Kerr *et al.*, "Optical pyrometry for gas turbine aeroengines," *Sensor Review*, Vol 24, No. 4, 378-286, Emerald Group Publishing Limited (2004)

[9] C. Yeh., *Handbook of Fiber Optics: Theory and Application*, Academic Press, Inc, Ann Arbor, Michigan, 1990

[10] D.A. Krohn., *Fiber Optic Sensors: Fundamentals and Applications.*, Instrument Society of America, North Carolina, 1992.

[11] Y. Alayli et al., "Applications of a high accuracy optical fiber displacement sensor to vibrometry and profilometry," *Sensors and Actuators* A **116** (2004)

[12] Kazuro Kageyama *et al.,* "Smart marine structures: an approach to the monitoring of ship structures with fiber-optic sensors," *Smart Mater. Struct.* **7** 472-478, (1998)

[13] D.W. Ball., "Field Guide To Spectroscopy," *SPIE Press*, Bellingham, WA (2006)

[14] http://www.physicsanimations.com/sensors/english/img002.gif

[15] http://www.optics4kids.com/terms/instruments.html

[16] A. Dandridge et al., "Homodyne Demodulation Scheme for Fiber Optic Sensors Using Phase Generated Carrier," *IEEE Journal of Quantum Electronics*, Vol. QE-18, No. 10, (1982)

[17] K.T.V. Grattan et al., "Fiber optic sensor technology: an overview," *Sensors and Actuators A: Physical*, vol.82 iss.1-3 (2000)

[18] "SOFO® Technology," *Smartec SA*, Switzerland (2006)

[19] http://www.polytec.com/default.asp

CHAPTER 3: DEVICE FABRICATION AND EXPERIMENTAL APPLICATION

Now that it has been shown in Chapter 2 why the Michelson Interferometer has been chosen to be used in this research as a vibration sensor, this Chapter will serve to describe the design considerations that were made in the production of four prototypes. Following that, the experimental set-up and application of the sensor will be described.

3.1 Fiber Optic Michelson Interferometer Vibration Sensor Fabrication

As described in Section 2.2.4 of this thesis, the Michelson interferometer is a phase modulated based sensor and was the system of choice for the design of our vibration sensor. Figure 3.1 shall be used in order to define the terms to be used to describe our device fabrication and application. L_1 and L_2 are the two arms of the Michelson interferometer respectively. The coupler is used so that light coming in from the source is split into both arms and then upon its reflection through the coupler is diverted toward the detector rather than back to the source [1]. The source and detector used in our experiments will be described in more detail in Section 3.4.

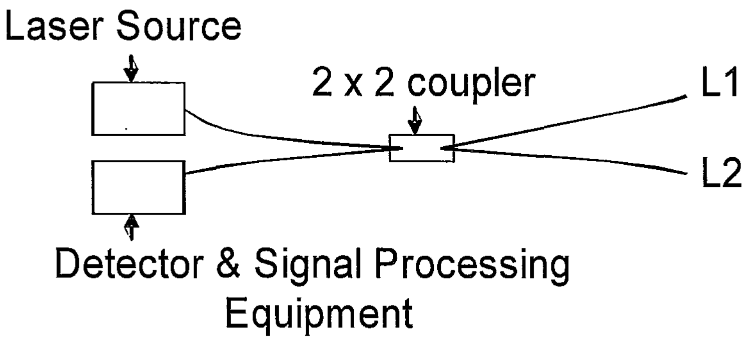

Figure 3.1. Global layout of the Fiber Optic Michelson Interferometer Vibration Sensor

Throughout the course of testing for this fiber optic vibration sensor a few different prototypes were designed to package and house the optical components of the sensor. Each of these packaging designs will be described in this Chapter. It is important to note, however, that the conceptual approach with respect to the optical elements in the sensor did not change other than the occasional fine-tuning of fabrication procedures here and there to improve the efficiency and overall robustness of the system. All four prototypes fabricated for this thesis used a flexible cantilever with L_1 and L_2 (see Figure 3.1) wound and secured to the top and bottom respectively of the disc[4] (see Figure 3.2).

[4] Of the four fabricated cantilevers two were discs and two were rectangular shaped. I will hereto in the following paragraphs refer only to 'disc' in reference to the cantilevers for simplicity's sake. Specific differences in the two types will be identified in the discussion of the prototypes individually in Section 3.3 and in other parts as required.

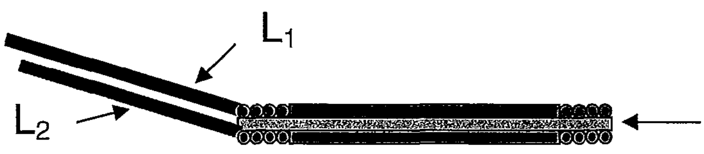

Figure 3.2. Illustration of transparency disc (gray) with the interferometer arms (L_1 - pink and L_2 - blue) coiled and attached to either side of the disc.

When the vibration sensor is under acceleration, the cantilever deflects up and down because of inertia. The deflection of the cantilever is in the opposite direction from the acting acceleration and the amplitude of that deflection is proportional to the acceleration [2]. As the cantilever bends, the optical fibers coiled on either side of the cantilever move relative to each other (i.e. the optical path length of the top fiber lengthens as the other shortens when the cantilever deflects downward and vice versa when the cantilever deflects upward).

The first step in creating the device is to prepare the winded fiber disc. A small disc was cut from a clear transparency with an additional hole cut in the center for mounting the disc later. The two fiber arms, L_1 and L_2, were measured out to approximately one meter and cleaved within mm of each other[5] [3]. In order to prevent the fiber tip from breaking later, it is important to cleave the fiber very close to the fiber jacket [4]. Before the winding is carried out, the silver mirrors must be added to the fiber arm tips. The silver mirror reaction procedure is outlined in detail in Section 3.2 [5].

[5] The actual optical path length difference was calculated through experimental results for Prototypes #3 and #4. These results are detailed in Section 3.3.3

One fiber arm of the interferometer was delicately wound on each side of the disc (see Figure 3.2). Small strips of double sided tape were used to secure the fiber to the disc as it was being wound. Once the coiling was complete, both sides of the disc were coated with a thin layer of Epo-tek 353ND heat cure epoxy to further secure the fiber coils and offer a little more rigidity to the overall disc [3].

Next the remaining loose fiber extending from the wound fiber disc was carefully spliced to a single-mode wideband fiber coupler. Once the splices were complete, each splice was coated and covered with a mini fusion splice sleeve to protect the fibers and the splice [3].

When assembling Prototype #2, the disc was secured to the stainless steel holder before the splicing with the coupler was complete [3]. For Prototype #3, the disc was secured to the housing after it was spliced to the coupler.

3.2 The Silver Mirror Reaction

The procedure described below was used to make the silver mirrors and was in line with the procedure titled "Tollen's Test" described by David A. Katz [5]. The materials required to create the silver mirrors for the fiber tips are as follows:

Solutions:

- Silver nitrate, $AgNO_3$;
- Potassium hydroxide, KOH;

- Dextrose, $C_6H_{12}O_6$;
- Ammonia, NH_3; and
- Nitric acid, HNO_3.

Apparatus:

- Small glass container with lid;
- Conical bottom tube with stopper;
- Graduated pipettes; and
- Analog vortex mixer.

Since mixtures of $AgNO_3$, NH_3, and KOH will form an explosive precipitate if they are allowed to stand, as a safety precaution, the reagent used to make the mirrors was prepared fresh each time a new interferometer was required.

The following paragraphs detail the steps taken to prepare the silver mirrors.

Place 10 mL of $AgNO_3$ solution in a 150 mL conical bottom tube. Add concentrated NH_3 drop by drop, using the mixer to stir with each drop, until the brown precipitate just dissolves. Add 7 mL of the KOH solution. If the brown precipitate returns, continue adding more concentrated NH_3 drop by drop, until it dissolves.

Add 2 mL of $C_6H_{12}O_6$ and the previous solution into the glass container and screw on the lid. Use the mixer to shake the container so that the liquid comes in contact with the whole inner surface of the flask. After approximately one minute, the silver mirror starts to form. Carefully take the lid off and place the cleaved fiber ends inside the glass container and hold them steady for about five minutes until the flask has a complete silver mirror coating. Then clean the mirror tips that have formed on the cleaved fiber ends with ethanol.

To protect the freshly made mirrored fiber ends, coat them with Epo-tek 353ND heat cured epoxy.

3.3 Mechanical Design of the Fiber Optic Michelson Interferometer Vibration Sensor Prototypes

There were four prototypes fabricated throughout the course of these experiments. Each one will be detailed in the subsequent paragraphs. The following list provides a quick overview of each sensor:

3.3.1 Prototype #1 – elongated cantilever (rectangular), standard single mode fiber, no external packaging;

3.3.2 Prototype #2 – circular cantilever disc, bending insensitive fiber, most sophisticated packaging design;

3.3.3 Protoype #3 – circular cantilever disc, bending insensitive fiber, small gray box packaging; and

3.3.4 Prototype #4 - elongated cantilever (rectangular), standard single mode fiber, large black box packaging.

3.3.1 Prototype #1

Prototype #1 was the original proof of concept design carried out by a previous member of our research group, Jian Yang [3].

The interferometer arms, L_1 and L_2, were made of standard single mode fiber that was wound in an elongated oval onto a rectangular transparency cantilever (instead of a disc cantilever). Figure 3.3 is a photo taken of Prototype #1 mounted on the shaker table used for experimental results.

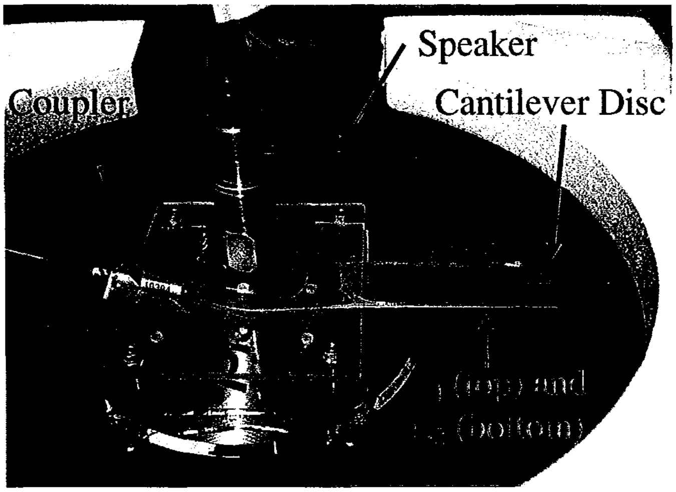

Figure 3.3 Prototype #1, original proof of concept design [6]

3.3.2 Prototype #2

Since the two fiber arms, L_1 and L_2, are to be wound or coiled around the disc (like a race track), we decided to use bending insensitive fiber to minimize the loss effects from bending the fiber [3].

Prototype #2 was the most sophisticated packaging design of the four manufactured prototypes and it was prepared using bending insensitive fiber for the disc cantilever. This packaging was designed and manufactured specifically with the Hot Mill environment in mind [6].

It had a screw protruding from the bottom of the device that was used to attach the device to a magnet. In turn, this magnet was to be used to mount the device on machinery in the mill along the desired axis direction to be measured as required.

Figure 3.4 is an illustration of the internal design of the vibration sensor housed in its external packaging and Figure 3.5 is a picture of the completed Prototype #2 mounted on the shaker table.

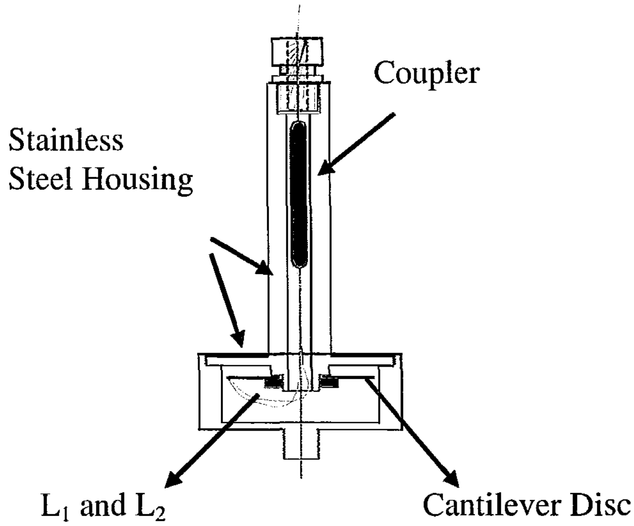

Figure 3.4. Prototype #2 with robust packaging and compact design. The fiber coil disc is located inside the chamber at the bottom of the figure while the coupler is mounted and secured with epoxy inside the longer cylinder [6].

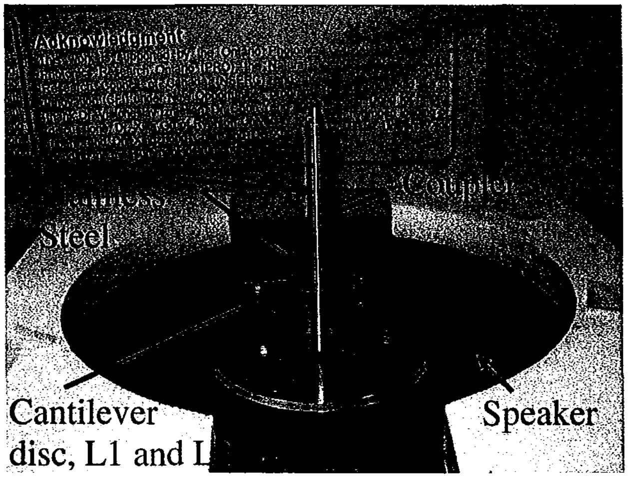

Figure 3.5. Photo of Prototype #2 mounted on the shaker table during testing [6].

Even though Prototype #2 was the most sophisticated packaging design, it proved very difficult to secure the sensor itself inside the housing. The areas were very small and the room for splicing error was next to nil. In fact, despite the robust nature of the housing itself, we ascertained that Prototype #2 was too fragile to continue working with and as a result Prototypes #3 and #4 were packaged inside metal boxes.

3.3.3 Prototypes #3 and #4

The major difference between the Prototype #3 and #4 is that Prototype #3 (see Figure 3.6) was manufactured using bending insensitive fiber whereas Prototype #4 (see Figure 3.6) was manufactured using standard single mode fiber instead. Since Prototype #4 did not have bending insensitive fiber in the coil (similar to Prototype #1), there was no requirement to splice the coiled fiber to the coupler. Instead the fiber arms directly from the coupler were used to do the winding. The box used for housing Prototype #3 is smaller than that used for Prototype #4 as well.

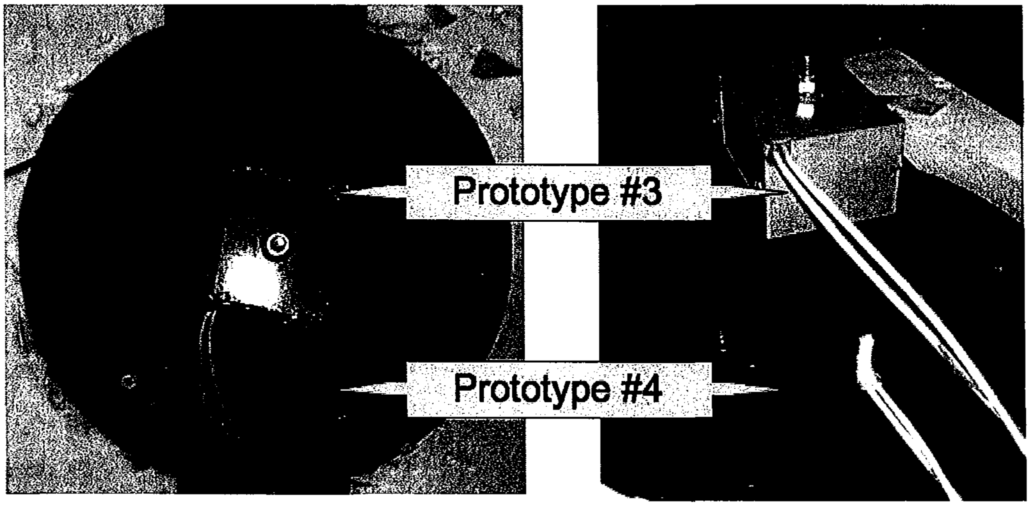

Figure 3.6. Photo of Prototype #3 (gray box) and Prototype #4 (black box). Left photo is top down view. Right photo is side view.

3.3.3.1 Optical Path Length Difference Calculations

The optical path length difference between the two interferometer arms, L_1 and L_2, help determine the dynamic range of the sensor since mathematically, the optical phase delay is given by,

$$\phi = nkL \qquad \text{(Equation 3.1)}$$

where n is the index of refraction of the fiber core, k is the optical wavenumber ($\kappa = \frac{2\pi}{\lambda}$), and nL is the optical path length (L was previously defined in Equation 1) [7]. Referring again to Figure 2.16, the sensitivity of the interferometer varies with the relative phase between the two light beams, or arms L_1 and L_2 [1].

We are able to calculate the optical path length difference numerically using the results from a scan on the tunable laser. Without any input vibration, we scanned the laser wavelength from 1550 nm to 1552 nm with steps of 3 pm. The wavelength value of the output signal was measured at four integrals of 2π (see Figure 3.7).

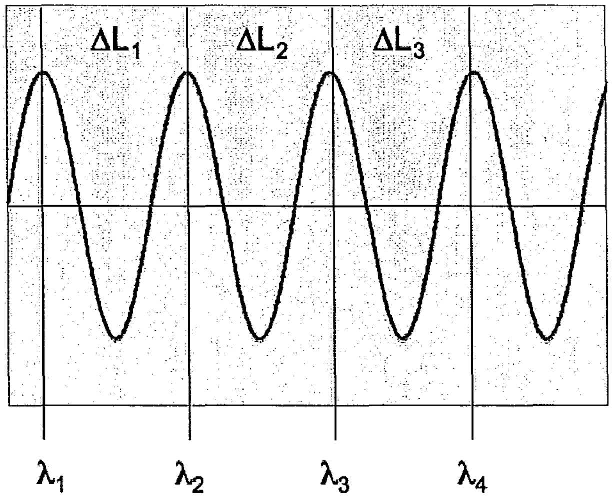

Figure 3.7 Illustration of the method used to calculate the optical path length difference between L_1 and L_2 [8].

These values labelled λ_1 through λ_4 (see Figure 3.6) were used in the following equation to calculate each of the values of ΔL:

$$\Delta f = \frac{2pn\Delta L_1}{\left[\left(\frac{1}{l_1}\right)-\left(\frac{1}{l_2}\right)\right]} \qquad \text{(Equation 3.2)}$$

where $\Delta\phi$ is equal to 2π (in other words, the wavelength values are measured from peak to peak at intervals of 2π). To find the overall optical path length difference[6], ΔL, an average of ΔL_1, ΔL_2, and ΔL_3 (see Figure 3.7) was taken [8]. For Prototype #3, the calculated optical path difference was 4.629 mm and for Prototype #4 it was 4.946 mm.

3.4 Experimental Arrangement of the Fiber Optic Michelson Interferometer Vibration Sensor and Test Bench

The experimental set-up of the fiber optic Michelson interferometer vibration sensor is schematically shown in Figure 3.8.

The realization of the experimental set-up for our fiber optic Michelson interferometer vibration sensor required the assembly of seven main components besides the sensor itself.

[6] Since this is a Michelson interferometer, the optical path length difference calculated takes into consideration the second pass of the reflected beam.

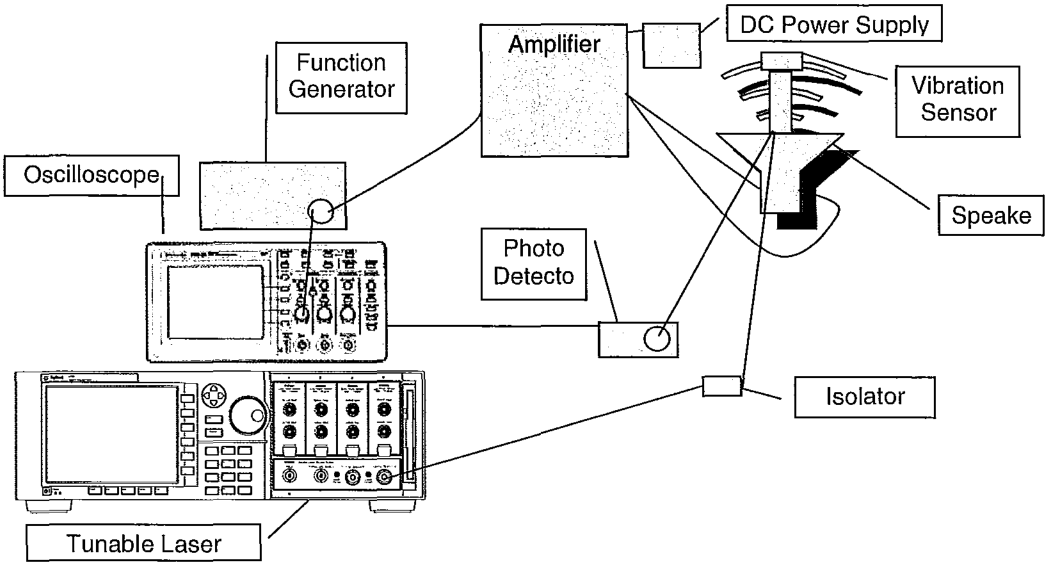

Figure 3.8. Schematic diagram of the fiber optic Michelson interferometer vibration sensor experimental set-up [3]

Light Source

The laser source used for the lab test bench was the Agilent Technologies Tunable Laser module. It allowed the laser source wavelength to be varied through a specific range in order to select the optimized wavelength based on the output power from the sensor. The output signal from the tunable laser diode centered on a wavelength near 1550 nm.

Isolator

The light from the tunable laser was injected into a JDS Uniphase isolator and sent to the fiber optic Michelson interferometer vibration sensor. The isolator was inserted into the set-up to minimize any back reflection into the laser.

Function Generator

In order to create the waveforms necessary to vibrate the sensor, the HP 33120A 15 MHz synthesized function generator was used. Figure 3.9 is a diagram of the function generator front panel. The function generator was used to modify the waveform's frequency and amplitude in order to vary the vibration spectrum influencing the fiber optic vibration sensor [8]. It was my experience that the best results arose when the minimum amplitude of 50 mV peak to peak was selected.

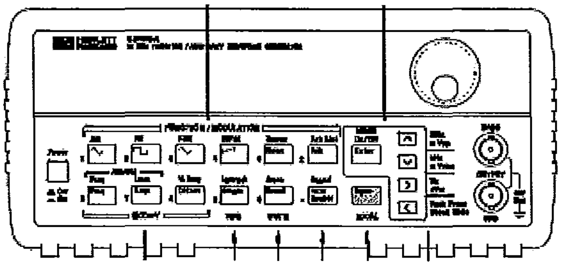

Figure 3.9. Function Generator front panel [8].

Amplifier

An MTX Thunder TC2002 Audio amplifier was used to transfer the electrical into audio power to the speaker, which was used as a shaker table [3].

Shaker Table

The sensor was mounted on the shaker table, which is identified in Figure 3.5 as "speaker" since it is actually a Pioneer 12" 4Ω subwoofer. An overview of the shaker table is illustrated in Figure 3.10.

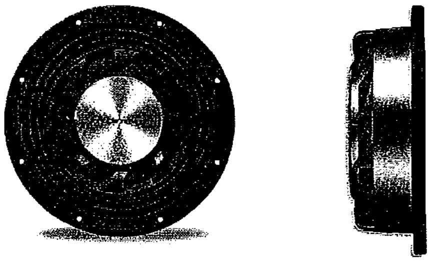

Figure 3.10. Pioneer 12" 4Ω subwoofer, top view (left) and profile view (right), used as a shaker table for experimental set-up [9].

Photodetector

The light reflection from the fiber optic Michelson interferometer vibration sensor was transmitted to the Thorlabs PDA10CS InGaAs Amplified Photodetector. The photodetector had switchable gain which provided us with the ability to adjust the gain and take full advantage of the photodiode response range. Gains were adjustable in eight 10dB steps.

Oscilloscope

From the photodetector, the signal was subsequently read and recorded on the oscilloscope, which in this case was a LeCroy Waverunner Model LT224. The optical spectrum data that was collected and saved in binary from the oscilloscope was copied to a disk and loaded onto a computer, converted into ASCII, and then exploited for post-experiment study using a data analysis program, like Origin®.

References for Chapter 3

[1] E. Udd., "An overview of fiber-optic sensors," *Rev. Sci. Instrum.* 66 (8), (1995)

[2] J. Kalenik, R. Pajak, "A cantilever optical-fiber accelerometer", Sens. Actuators A: Phys. 68 (1-3) (1998) 350–355.

[3] Private communications with Dr. Jian Yang (2008)

[4] http://www.tpub.com/neets/tm/108-3.htm

[5] D.A. Katz., "The Silver Mirror Reaction (Tollen's Test)," University of Wisconsin-Madison, (2002)

[6] C.Q. Xu *et al.*, "Progress of FOS for Monitoring of Vibration," submitted for presentation to ArcelorMittal Dofasco (2008)

[7]. E. Udd., *Fiber Optic Sensors: An Introduction for Engineers and Scientists*, A Wiley-Interscience Publication, 1990

[8] Private communications with Dr.Yong Wang (2009)

[9] "HP 33120A/Function Generator / Arbitrary Waveform Generator: User's Guide," Hewlett-Packard Company (1997)

[10] http://www.crutchfield.com/S-6ESGOeFUb09/p_130TSS3041/Pioneer-TS-SW3041D.html

CHAPTER 4: EXPERIMENTAL RESULTS OF THE FIBER OPTIC MICHELSON INTERFEROMETER VIBRATION SENSOR PROTOTYPES

In this Chapter, the study of four fiber optic Michelson interferometer vibration sensor prototypes is demonstrated. It is shown how changes in the surrounding area, which are controlled through operation of the shaker table or in certain cases were invoked through the normal operations at the Hot Mill, affect the sensitivity of the prototypes. The experimental setup is schematically shown in Figure 3.7. In all cases, the primary measurand of interest is the vibration frequency spectrum at very low frequencies.

4.1 Prototype #1

The first device that we will discuss here is Prototype #1. The purpose of Prototype #1 was to prove the original design concept only and was never intended for use in the Hot Mill. Consequently there was no requirement to externally package the device. Experimental results from Prototype #1 and #2 were the original work done primarily by Dr. Jian Yang in our research group [1]. A selection of his results is illustrated in Figure 4.1. The red waveform illustrates the vibration signal. The black waveform was recorded after the vibration signal was sent through Prototype #1. It is clear from Figures 4.1a through d that the period illustrated in Prototype #1's waveform coincides with that from the input signal. The change in amplitude of the black waveform is an indication in the change in amplitude of the vibration sensor. The distortion of the black waveform most likely occurs because the signal travels through 2π many times.

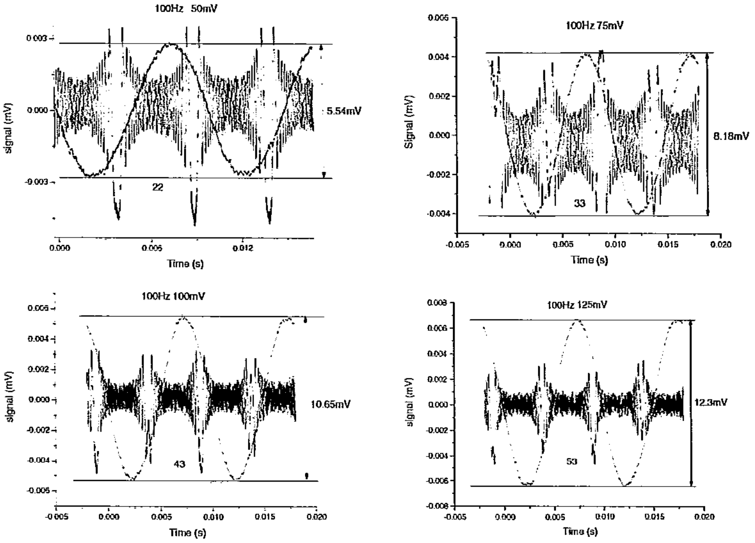

Figure 4.1. Comparison graphs of Prototype #1 (black) to a traditional piezoelectric sensor (red) [1].

4.2 Prototype #2

The next step in the development was Prototype #2, which was the most sophisticated of all four prototypes in terms of packaging and the most complicated in terms of assembly. Unfortunately, Prototype #2 was broken before extensive results could be recorded in the lab. However, one very interesting test was done that was not carried out on any of the other sensors. Prototype #2 was placed on the basement floor of the laboratory located in CRL

B110/C at McMaster University. The results from that experiment are illustrated in Figure 4.2 and Figure 4.3 [1]. From these results it is easy to see the potential sensitivity of this sensor design. Since the basement floor motion is small, the phase shift did not go over 2π. As will be seen, the best results we achieved were when we could be quite certain this was the case. When the phase shift between the two arms is on the "close to linear" section of the sine wave, the sensitivity of the sensor is at its highest [2].

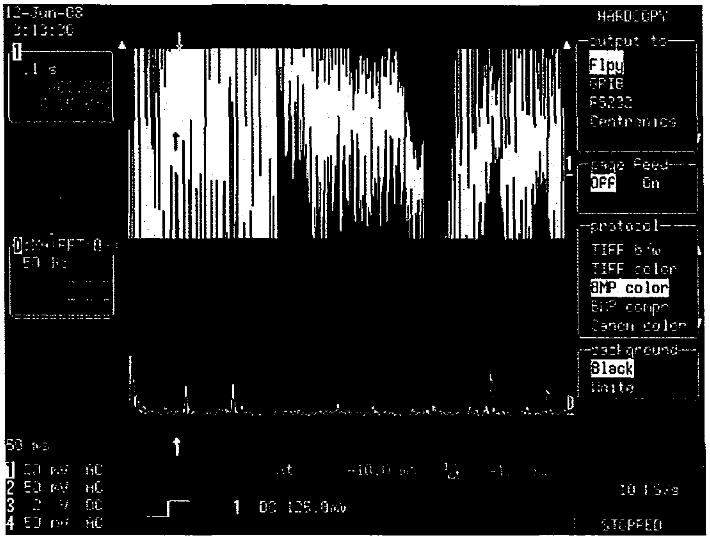

Figure 4.2. Snapshot of the output signal from Prototype #2 (top) and the FFT of that output (bottom) [1]

The full range of frequency of the Fourier Transform in Figure 4.3 is 0 – 50 Hz. The lowest signal is 6-7 Hz, could be the vibration frequency of the Earth itself [3] and the signal at 12 Hz could be the second harmonic.

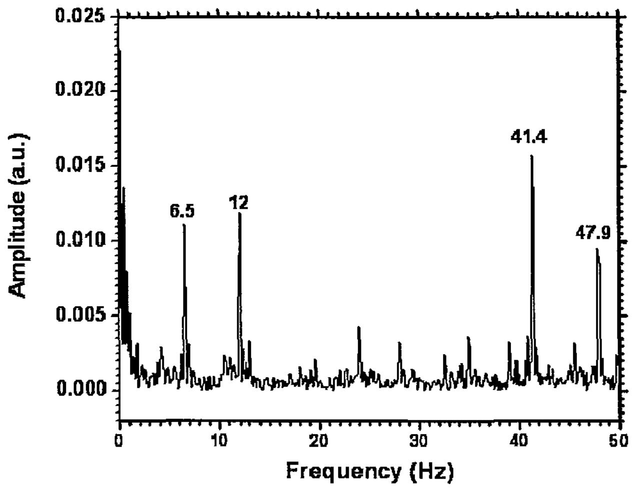

Figure 4.3. Graphical representation of the FFT of the output signal of Prototype #2 when placed on the basement floor of the laboratory located in CRL B110/C at McMaster University [1].

Kevin Hunt, who is a specialist on the Hot Mill Health and Safety Committee at ArcelorMittal Dofasco, confirmed for us that the vibration "footprint" created from the heavy industry in Hamilton is about 47.9 Hz and is frequently referred to as the "bayfront signature" in the industry [4]. The "bayfront signature" is a combination of all the heavy machinery working. The steel mills are located at the "bayfront" and are approximately 8-10 km from McMaster University [5]. The signature may be slightly different if verified since as of the date we finished collecting data one of the two major steel plants in Hamilton, US Steel (also known as Stelco) has been shut down. That said, news reports indicate they may restart the blast furnace and continue production in the near future as demand for steel is rising [6]. Unfortunately Prototype #2 broke shortly after being first tested and could not be used for further comparison experiments.

In general, the 42 Hz range is used as the common background at the Hot Mill at ArcelorMittal Dofasco. The 41.4 Hz peak is unique to the two hi-stand reversing roughers [4].[7]

The smaller peaks in around the 20-30 Hz range are most likely due to mankind in some fashion, i.e. HVAC, waterflow, traffic, etc. The particulars of where the vibration detected in that frequency range was coming from was not explored as a part of this thesis.

Unfortunately we do not have much data from Prototypes #1 and #2. Prototype #1 was not tested at great length and Prototype #2 was broken before a lot of data could be collected. Since we did not have much time before the field testing was set to begin, we opted for a less sophisticated packaging design with Prototype #3 but it did have the same sensor layout as Prototype #2 (circular race track cantilever for interferometer arms). Since bending insensitive fiber and the circular race track cantilever were used, the packaging was still quite compact, especially when compared to Prototype #4.

[7] On the particular day that these measurements were taken, the rougher was being run at half speed, i.e. only one steel piece was in the mill at a time. Normally there can be up to three pieces in the mill, one coming out of the reheats, one at the rougher, and one in the finisher coiler area.

4.3 Prototype #3

As detailed in Section 3.3, Prototype #3 was manufactured using bending insensitive fiber and then packaged inside a metal box. Prototype #3 was tested on site at ArcelorMittal Dofasco in many different locations. Figure 4.4 is a layout diagram of one of the testing locations. Figures 4.5 is a comparison example of the results from our Prototype #3 and a device designed by another research group under the supervision of Dr. Paul Jessop. The results from the two sensors are similar. In our group, we are mostly concerned about the results that indicate the fundamental frequency at 100 Hz but also the second harmonic at 200 Hz. A 60 Hz peak is evident as well, which is most likely a result of electronic line noise [7] and its second harmonic at 120 Hz is also apparent.

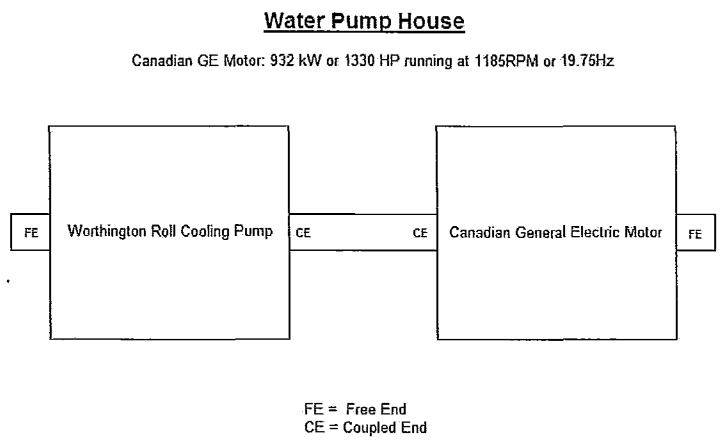

Figure 4.4. Top View of Water Pump House [8]

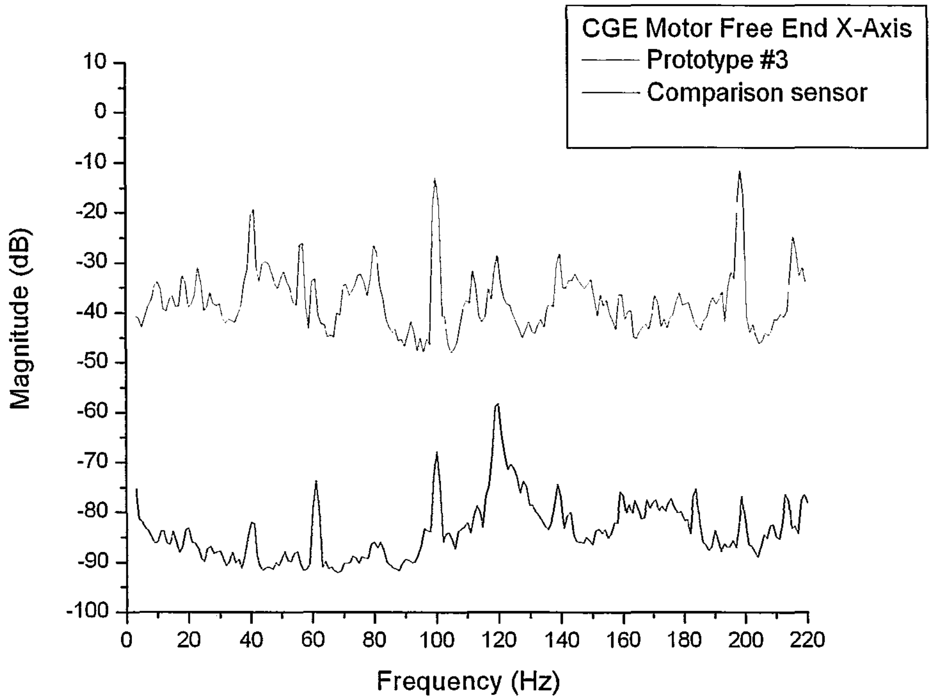

Figure 4.5. A graphical comparison of the results from our Prototype #3 sensor (Red) to the results from a sensor from another research group (Black). The area tested the free end of the Electric Motor of the Cooling Pump [8].

Prototype #3 was also tested in the lab using the set-up illustrated in Figure 3.7.

As discussed in Section 2.2.4 of this thesis, it is important to operate in the region of a ¼ wavelength shift where the rate of change of intensity with phase shift is greatest since this is the area of most sensitivity [2,9]. Before the experiments on Prototype #3 and #4 were started, a power meter was connected to the tunable laser and a Passive Component Test, or PACT, was carried out in order to sweep the laser across a pre-determined set of wavelength parameters in order to determine the wavelength at which the sensor allows the most power at output [10]. In other words, the result of the PACT shows the maximum laser output power for the tuneable laser across the selected wavelength range. An example of the PACT set-up screen is shown in Figure 4.6. The wavelength selected for testing Prototype #3 was 1550.0407 nm.

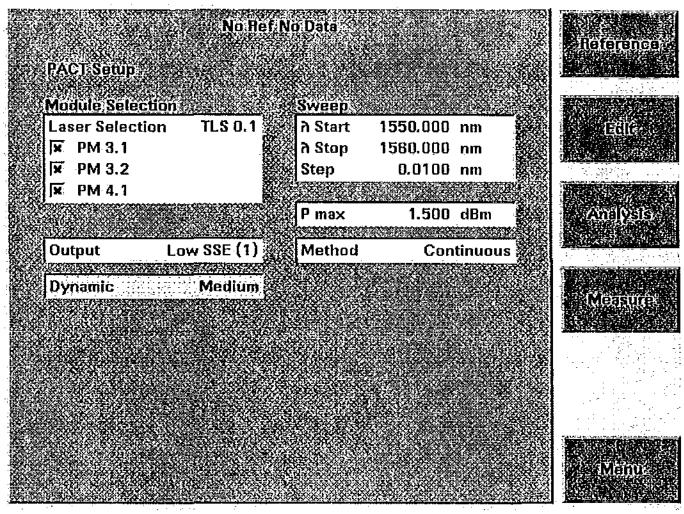

Figure 4.6. An example of the set-up screen for the PACT (Passive Component Test). This test makes it possible to select a wavelength that maximizes the power output through the connected sensor [10].

Samplings of the full set of results from Prototype #3 are presented in Figures 4.7a through 4.7d. The fundamental vibration frequency is sensed by the Prototype in each case. However, the output also includes the harmonic information, which in the case of our operational requirements at ArcelorMittal Dofasco, is perceived as noise that makes this Prototype impractical. This harmonic 'noise' is most likely a result of the signal passing through 2π on more than one occasion. As we saw earlier in Figure 4.3, when the amplitude is very small, such that the signal does not pass through 2π, the output is very precise. In the same fashion, in order to minimize this unwanted harmonic information in the output of Prototype #3, the sensor needs to be optimized in such a fashion as to keep the signal from passing through 2π since it is impossible to limit the vibration detected in the field to a lower amplitude – after all, it is what it is.

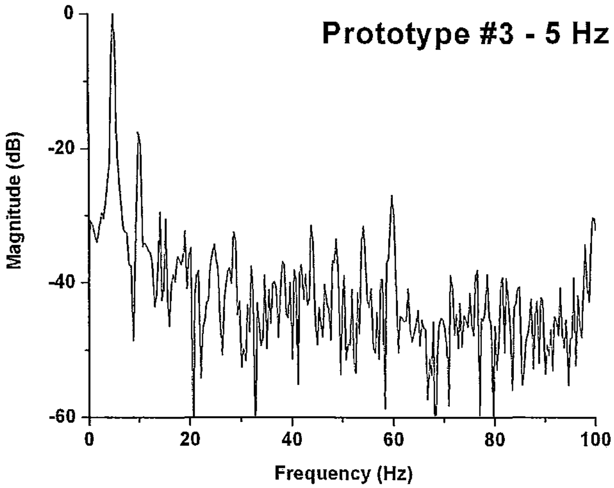

Figure 4.7a. Graphical representation of the FFT of the output signal of Prototype #3 when shaken at 5 Hz.

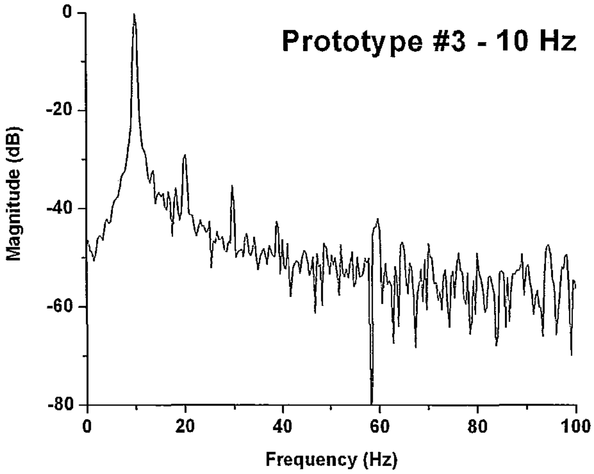

Figure 4.7b. Graphical representation of the FFT of the output signal of Prototype #3 when shaken at 10 Hz.

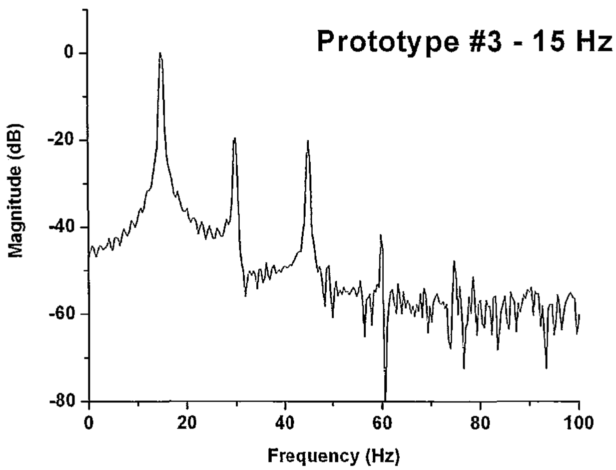

Figure 4.7c. Graphical representation of the FFT of the output signal of Prototype #3 when shaken at 15 Hz.

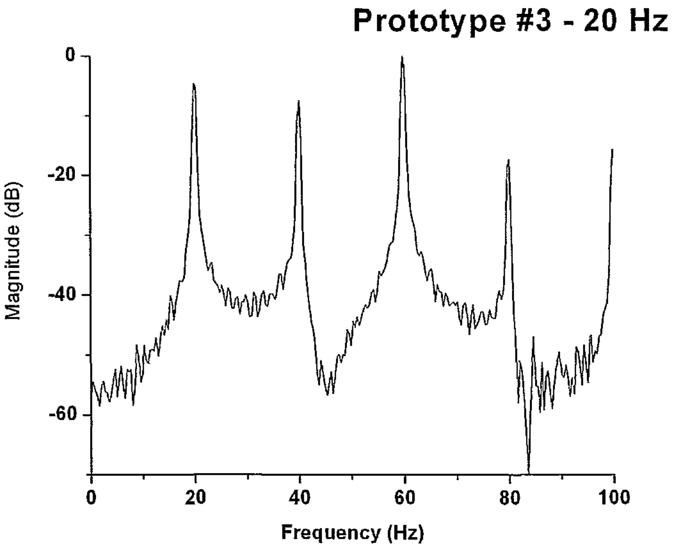

Figure 4.7d. Graphical representation of the FFT of the output signal of Prototype #3 when shaken at 20 Hz.

In order to more precisely characterize the performance of the sensor, we decided to determine a figure of merit to validate whether or not the sensor has any utility at particular frequencies [11]. We define the figure of merit, of FOM, as:

$$FOM = P(f_o)/\Sigma P \qquad \text{(Equation 4.1)}$$

where P is power [12]. According to the FOM for Prototype #3, which is graphically represented in Figure 4.8, the sensor performance is much less reliable above 17 Hz.

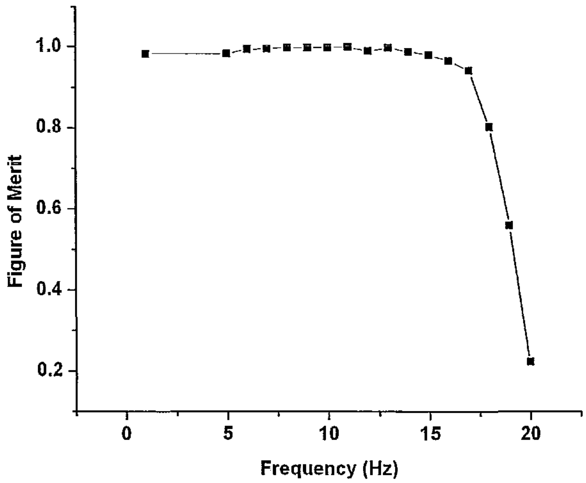

Figure 4.8. Graphical illustration of the Figure of Merit for Prototype #3 [12].

4.4 Prototype #4

For Prototype #4, the wavelength selected was 1550 nm. Samplings of the full set of results from Prototype #4 are presented in Figures 4.9a through 4.9c. Unlike Prototype #3, the fundamental vibration frequency is not necessarily sensed by the Prototype in each case. In fact, in most cases the second harmonic signal is more apparent than the fundamental. As a result, the results from these tests show that Prototype #4 is even more impractical for our operational requirements at ArcelorMittal Dofasco.

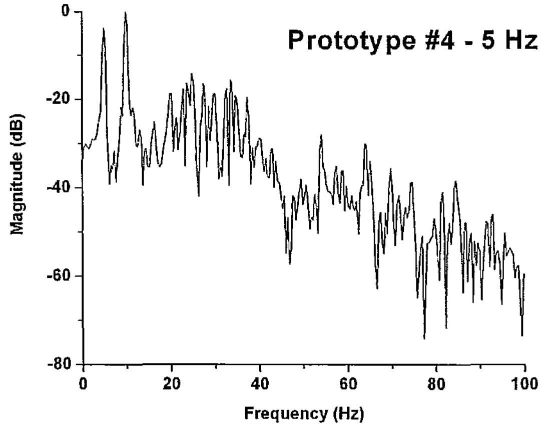

Figure 4.9a. Graphical representation of the FFT of the output signal of Prototype #4 when shaken at 5 Hz.

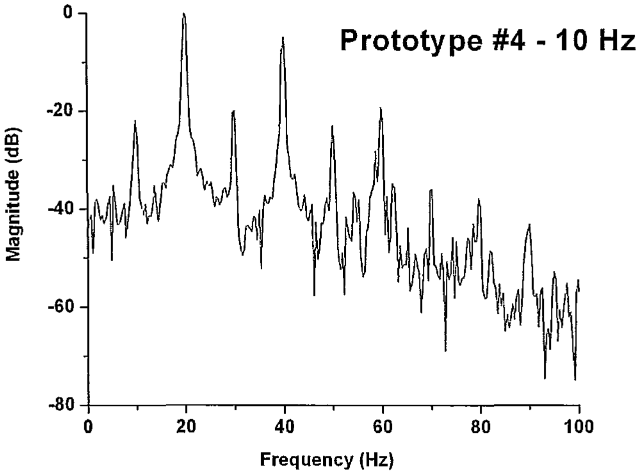

Figure 4.9b. Graphical representation of the FFT of the output signal of Prototype #4 when shaken at 10 Hz.

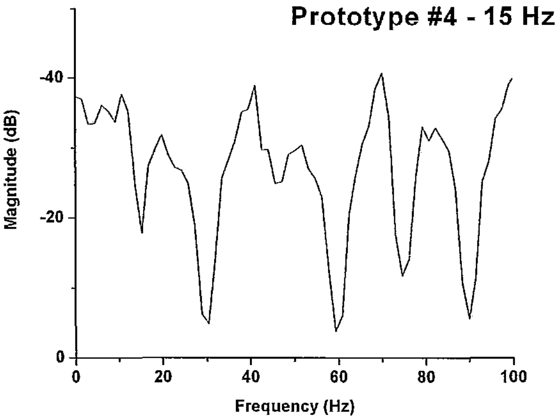

Figure 4.9c. Graphical representation of the FFT of the output signal of Prototype #4 when shaken at 15 Hz.

According to the FOM for Prototype #4, which is graphically represented in Figure 4.10, the sensor performance is much less reliable at all frequencies than its predecessor Prototype #3. This is to be expected since Prototype #4 was not made with bending insensitive fiber like Prototype #3 so optical losses would have been greater. Also, the cantilever used in Prototype #4 is an elongated, or rectangular, cantilever.

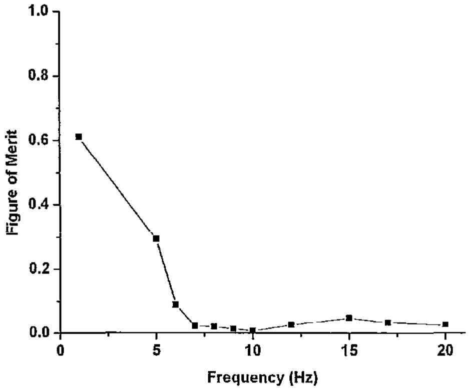

Figure 4.10 Graphical illustration of the Figure of Merit for Prototype #4 [12].

References for Chapter 4

[1] C.Q. Xu *et al.*, "Progress of FOS for Monitoring of Vibration," submitted for presentation to ArcelorMittal Dofasco (2008)

[2] E. Udd., "An overview of fiber-optic sensors," *Rev. Sci. Instrum.* **66** (8), (1995)

[3] D.D. Stentman., "Electrical conductivity of Jupiter's shallow interior and the formation of a resonant of a resonant planetary-ionospheric cavity," Icarus **88**, (1990)

[4] Private communications with Kevin Hunt (2008)

[5] http://maps.google.ca/

[6] http://www.reuters.com/article/rbssIndustryMaterialsUtilitiesNews/idUSN2837758 62 0090828

[7] D. Radford., "Spread-spectrum data leap through ac power wiring," IEEE Spectrum, Vol 33, iss 11 (1996)

[8] B. Stoute., "Fiber optic temperature and vibration sensors," McMaster University, (2008)

[9] D.A. Krohn., *Fiber Optic Sensors: Fundamentals and Applications.*, Instrument Society of America, North Carolina, 1992.

[10] "Agilent 8163A/B, 8164A/B & 8166A/B Mainframes", Sixth Edition, Agilent Technologies, Germany, 2004.

[11] H.J. Arditty et al., *Optical Fiber Sensors.*, Springer Proceedings in Physics **44** (1989)

[12] Private communication with Dr. Yong Wang (2009)

CHAPTER 5: CONCLUSIONS AND CONSIDERATIONS FOR FUTURE WORK

The previous Chapters of this thesis investigated fiber optic vibration sensors. In summary, there were two complimentary goals of this research. The first objective of this work was to develop a fiber optic vibration sensor that could withstand the harsh environment of the Hot Mill used for steel production and the second objective was to use that sensor to detect low frequency vibration and from the data collected from measuring this vibration produce plots of the frequency spectrum produced from applying an FFT. In this regard, the main contributions of this project are presented in the following paragraphs.

5.1 Review of Lessons Learned and Conclusions

The field tests carried out at ArcelorMittal Dofasco did serve to illustrate the robustness of the packaging and survivability of the sensor itself. There were large shocks in the surroundings of the sensor when the steel passed under the power house and it is an incredibly hot and dirty venue. Despite that, the sensor was not damaged in any way. In addition to illustrating the sturdiness of the sensor, the field tests taught us a lot about how to use the device and entire set-up for field testing [1].

It can be concluded from the selected results presented in Chapter 4 that the fiber optic vibration sensors developed in this group is sensitive to changes in vibration at low frequencies, from 1 to 16 Hz. The prototypes that showed the best sensitivity were those that utilized the cantilever disc design with bending insensitive fiber.

Future work is required to eliminate all the extraneous information resulting from the occurrence of harmonic frequencies.

5.2 Future Work: Suggestions for Improvement of the Current Fiber Optic Vibration Sensor Design

In order to produce better results the properties of the cantilever need to be characterized well. In order to do this, one must carry out two types of study: a mechanical study and an optical study. The following is a list of future work that should be done in attempt to further improve the overall design and performance of the sensor:

1. The mechanical study involves examination of how the longitudinal dimensional change, ΔL, relates to the acceleration to be measured [2]. For the mechanical study, one must consider the selection of material for the cantilever itself. Therefore, the simplest extension of this work would be to carry out further experiments on materials with varying Young's Modulus of Elasticity to determine the most suitable stiffness of material

required and to determine how the change in cantilever stiffness affects the overall device sensitivity [3]. Once an optimized material is selected it would be worthwhile knowing the fatigue limit of the cantilever since the eventual goal is to exploit it operationally as part of a preventative maintenance program in the steel mill. This increases the complexity of fabrication in the short term but would likely result in extremely high sensitivity enhancement in the long term.

2. Again for the mechanical study, in addition to examining the stiffness of the cantilever, the resonant frequency of the cantilever and saturation point should be examined as well, so that the operator will know more about at what frequency is the output from the sensor inaccurate. This will improve the knowledge about the operating parameters of the sensor.

3. The optical study involves examination of how the optical phase shift is affected by the longitudinal dimensional change, ΔL [1]. In turn, this will help determine the linear range of the sensor such that it can be optimized for the specific application parameters.

4. Since the most precise results we achieved were found when the amplitude of the signal was very small (see Figure 4.3), and therefore did not travel through 2π, every effort should be made to ensure that any future testing be carried out within this operating parameter. This is easier

to achieve in the lab than in the field. Therefore, if further field tests are required, it would be worthwhile to carry out tests in the field to determine if the signal does travel through 2π and if so, how many times. If the results prove that this is the case then action must be taken to resolve the issue in order to produce the best possible results.

5. Automated fabrication techniques should be developed for assembling the fiber winding on the cantilever to maximize and standardize the device yield. An incredible amount of frustration could be avoided by using some sort of motorized stage for this part of the process. It would speed up fabrication time and would enable an increased ability to build and test different types of cantilevers as well.

6. Once a suitable system has been developed, the ideal next step would be to successfully build a system capable of being multiplexed [4]. Multiplexing the system should be a two-stage program. First, three unidirectional sensing elements, fixed orthogonal to one another, should be multiplexed together in order to measure the three directional components of the vibration signal [2]. Secondly, a profitable multiplexed system would consist of multiple three-component sensors located at some distance from the control and monitoring station to allow the end user to comfortably and more importantly, safely monitor the sensor outputs [1,4].

5.3 Future Work: Suggestion for Improvement of the Overall Fiber Optic Vibration Sensor Design

Since any improvements made to the sensor essentially mean starting over from the beginning anyway, I suggest consideration should be given to designing a completely new sensor. Given the work that has been completed during this thesis study, we now have a very good idea on how to proceed. The first step would simply be to pick a new sensor design and then carry out mechanical and optical studies before any field tests are carried out. My recommendation would be to go with one that is akin to the vertical seismic profile detection sensor illustrated in Ref [2]. In that particular case, the sensing element consists of elastic rubber cylinders wrapped with the two arms of a Michelson interferometer.

5.4 Final Remarks

Further to the results achieved while testing the four prototypes thus far, there is still much improvement required with respect to the design of the sensor and for the experimental processes. Much work remains to be carried out in order to realize a system that would be practical for use as a vibration monitoring and analysis tool for specific field application in the harsh environment of the steel mill where there is a lot of vibration aside from that being measured.

Notwithstanding the fact that the developed sensor does not work as well as we would have hoped, we still believe that potential exists for fiber optic vibration sensors to be very beneficial in the steel industry especially since this type of sensor can be multiplexed. This would significantly improve condition monitoring in the mill and reduce the complexity of the physical systems in situ at the mill.

There has been an incredible amount of research effort being put into fiber optic sensor development world-wide. It would not surprise me to find fiber optic sensors' dominating our every day lives in the not to distance future. Many already are without our even realizing it, from our car manufacturer to some of the devices used to monitor our health. These sensors have the ability to perform very accurate and sensitive monitoring and in this context, the steel industry (and those researchers that provide them with the technology) stands to benefit substantially if they are able to integrate them into their day-to-day operations.

References for Chapter 5

[1] Private conversations and work on-site at ArcelorMittal Dofasco under the supervision of Dofasco Coordinator, Kevin Hunt (2008)

[2] N. Zeng *et al.*, "A 3-component fiber-optic accelerometer for well logging," *Optics Communications* **234** (2004)

[3] S.E.U. Lima *et al.*, "Extrinsic and Intrinsic Fiber Optic Interferometric sensors for acoustic detection in high-voltage environments," *Optical Engineering* **48**(2) (2009)

[4] Private conversation with Dr. Chang-qing Xu (2008)